ROYAL OBSERVATORY, HONG KONG

Technical Note (Local) No. 61

# EPICENTRE DETERMINATION OF LOCAL EARTHQUAKES

by

SHUN Chi-ming

Published April 1992

Prepared by

Royal Observatory
134A Nathan Road
Kowloon
Hong Kong



550.34.06

# CONTENTS

# FIGURES

# TABLES

# 1. INTRODUCTION

In 1979, the Royal Observatory (RO) installed a network of three short-period seismographs to monitor earthquakes in the vicinity of Hong Kong. The stations, each equipped with a vertical-component high-gain short-period seismometer, are located at Yuen Ng Fan (YNF), Tsim Bei Tsui (TBT) and Cheung Chau (CC). Epicentres of local earthquakes were determined using a program developed in-house known as EPILOC. The program was later modified to work on personal computers (PCs) in 1987 and was renamed EPILOC87.

In 1988, an analysis on the accuracy of epicentre determination for local earthquakes using EPILOC87 was carried out (Ginn, 1988). In that study, it was concluded that if P-arrival times (P-times) from at least 4 stations were available, EPILOC87 could be used operationally to locate earthquakes up to a range of 70 km from the Royal Observatory Headquarters (ROHq) with percentage distance errors less than 25 %. Subsequently, a backup short-period seismometer was set up in the cellar at ROHq in 1989 using a spare seismometer and EPILOC87 could be executed operationally using P-times from ROHq, YNF, TBT and CC.

Ginn (1988) found out that epicentres obtained by EPILOC87 were not reliable for distances larger than 70 km (from ROHq), even when 4 P-times were available. As an example, for a locally felt earthquake which occurred at Heyuan in Guangdong, about 163 km north-northeast of ROHq on 25 November 1989, EPILOC87 located the epicentre at 34 km north (bearing = 11°) of ROHq using the 4 P-times as input. This implies a distance error of 129 km! As the earthquake actually occurred at more than 70 km away from ROHq, this large error is hardly surprising. However, judging only from the 4 P-times, we have no way to distinguish between an earthquake which occurred at Heyuan and one at about 34 km north of ROHq.

For earthquakes which occur within 70 km from ROHq, a 25 % distance error for EPILOC87 can mean distance errors in excess of 10 km. Because errors in assuming a constant P-velocity of 5.6 km/s and zero depth for hypocentres were not considered in Ginn (1988), the distance errors would be even larger in many cases.

In early-1990, an epicentre determination program known as HYPO71PC was purchased from the International Association of Seismology and Physics of the Earth's Interior (IASPEI) as part of an IASPEI Software Library (Lee, 1989). This program was originally known as HYPO71 and was developed by W.H.K. Lee and J.C. Lahr of the United States Geological Survey (USGS) in the early 1970's (Lee and Lahr, 1972 and 1975). It was extensively used for locating local earthquakes and was later modified to work on PCs (Lee and Valdes, 1985). It allows P- and S-times input and modelling of the crustal structure. Apart from computing the epicentral location, HYPO71PC can also determine the depth of the hypocentre.

In the following sections, formulation of the earthquake location problem will be discussed briefly. A method of analyzing the intrinsic errors pertaining to any location algorithm will be presented for small networks. The performance of HYPO71PC will then be compared with that of EPILOC87. Finally, actual seismic data obtained from earthquakes at Heyuan were used to test HYPO71PC further and the results will be discussed.

## 2. FORMULATION OF THE EARTHQUAKE LOCATION PROBLEM

For a small short-period seismograph network, its horizontal extent seldom exceeds several hundred kilometres and so curvature of the earth may be neglected and a Cartesian coordinate system (x,y,z) can be used in the earthquake location problem (Lee and Stewart, 1981). Suppose X, Y, Z, and T are respectively the coordinates of the hypocentre and the origin time for a given earthquake. The problem is to determine these 4 parameters given a set of arrival times (P- or S-times) $t_k$ from stations at positions $(x_k, y_k, z_k)$ (k = 1, 2, ..., n). For a given trial hypocentre $(X^*, Y^*, Z^*)$ and a trial origin time $T^*$, a set of theoretical arrival times $T_k$ (k = 1, 2, ..., n) can be obtained for a given crustal structure. Define

$$R = \Sigma_k (t_k - T_k)^2, \qquad k = 1, 2, \ldots, n \qquad (1)$$

as the residue which is a function of $X^*$, $Y^*$, $Z^*$ and $T^*$. The method (known as least squares approach) is to adjust the trial parameters such that the residue is minimized.

In EPILOC87, all hypocentres are assumed to have zero focal depth ($Z = Z^* = 0$ km), $z_k \approx 0$ km (k = 1 , 2, ..., n), and the P-velocity is a constant (5.6 km/s). It is therefore equivalent to assume a simple crustal structure with only one layer having P-velocity of 5.6 km/s. Furthermore, S-times are not considered in EPILOC87. Hence, the theoretical arrival times are given by :

$$T_k = T^* + \sqrt{[(X^* - x_k)^2 + (Y^* - y_k)^2]} / V_p,$$

$$\text{where } V_p = 5.6 \text{ km/s}, \qquad k = 1, 2, \ldots, n \qquad (2)$$

Instead of minimizing R, $R' = \Sigma_{i,j} (t_{ij} - T_{ij})^2$ is minimized (Poon, 1985), where

$$t_{ij} = t_i - t_j, \text{ and} \qquad (3)$$

$$T_{ij} = T_i - T_j, \qquad i,j = 1, 2, \ldots, n \qquad (4)$$

Thus, the terms $T^*$ are cancelled and the minimum residue is obtained by varying the trial parameters $X^*$ and $Y^*$ over all the vertices of a grid system. Optimal results were obtained for a system of three nested grids.

In HYPO71PC, the crustal structure is represented by a one-dimensional multi-layer velocity model, in which the crust consists of a sequence of horizontal layers. Each layer is characterized by a P-velocity and the depth to top of the layer. Up to 20 layers in the crust are allowed. The S-velocity for each layer is obtained by dividing the corresponding P-velocity by a constant factor (1.78 is recommended). For a given hypocentre, the theoretical arrival times $T_k$ (k = 1, 2, ..., n) can therefore be computed by applying Snell's law. To determine the hypocentre and origin time of an earthquake, HYPO71PC employs Geiger's method to minimize the residue R defined in Equation (1). In short, Geiger's method requires a first guess vector $(X_o, Y_o, Z_o, T_o)$ of the hypocentre and origin time. It then uses the Gauss-Newton iterative procedure to find a solution which minimizes R. In each iteration step i, a set of 4 simultaneous linear equations in 4 unknowns (known as a system of normal equations) is solved by a "stepwise multiple regression technique" (Lee and Lahr, 1975) and an adjustment vector $(\delta X_i, \delta Y_i, \delta Z_i, \delta T_i)$ is obtained to correct the vector $(X_i, Y_i, Z_i, T_i)$ so as to minimize R. When the adjustment is less than a certain critical value or when the number of iterations exceeds a given limit, then the iterative procedure stops and the final vector $(X^+, Y^+, Z^+, T^+)$ is taken to be the solution. Therefore, unlike EPILOC87, it is not necessary to compute the residue for every trial hypocentre (and origin time) which is extremely computer-time consuming for a multi-layer crustal model.

## 3. ERROR ANALYSIS OF THE EARTHQUAKE LOCATION PROBLEM

Before comparing the performance of HYPO71PC and EPILOC87, it is important to consider the intrinsic errors which will be present in any earthquake location method. Errors in earthquake location are inevitable due to the following causes :

(a) There are observational errors in determining the arrival times, and
(b) There are errors in the parameters which characterize the crustal structure (e.g., in EPILOC87, the assumption of a single horizontal crustal layer with a constant P-velocity is not realistic, as there are at least 2 layers in the crust - the granitic upper crust and basaltic intermediate layers (Bullen, 1963; Willmore, 1979), having different P- and S-velocities.

Of the above two causes, (a) can be examined in detail in the following paragraphs. To assess the effect due to (b), actual seismic data will be used to obtain quantitative estimates (see Section 6).

In manual seismogram analysis, it is usually possible to determine P-times to the nearest 0.1 s. Picking of S-times needs more skill to catch subtle changes in frequency and/or amplitudes in the seismic trace. Nevertheless, in general it is still possible to determine S-times to the nearest second. In analysis of digital seismic data collected by the IASPEI PC-based seismic data acquisition system (Lee, 1989) using a sampling rate of 100 Hz, an accuracy of up to 0.01 s can be achieved in phase picking.

Following SSB (1978), a method for error analysis of the earthquake location problem will be described. The following assumptions were made in the analysis due to limitations of computing resources and for direct comparison with the results obtained by Ginn (1988) :

(a) Focal depths are taken to be zero,
(b) The crustal structure is simplified by a single horizontal layer of constant P-velocity 5.6 km/s,
(c) The z-coordinates of the stations are zero, and
(d) $V_p/V_s = 1.78$

Now, when only P-times are considered, the travel time equation (2) can be written as :

$$(X^* - x_k)^2 + (Y^* - y_k)^2 = V^2(T_k - T^*)^2$$

$$k = 1, 2, \ldots, n \qquad (5)$$

where $V = 5.6$ km/s and $T_k$ ($k = 1, 2, \ldots, n$), are the P-times. Suppose there are errors $\Gamma_k$ in these P-times and the resulting errors for $X^*$, $Y^*$, and $T^*$ in solving Equation (5) are respectively $\alpha$, ß, and $\tau$, then

$$[(X^* + \alpha) - x_k]^2 + [(Y^* + ß) - y_k]^2 = V^2[(T_k + \Gamma_k) - (T^* + \tau)]^2$$

$$k = 1, 2, \ldots, n \qquad (6)$$

Expanding Equation (6), ignoring second order terms in $\alpha$, ß, $\tau$, $\Gamma_k$, and subtracting Equation (5), we obtain

$$(X^* - x_k)\alpha + (Y^* - y_k)ß = (T_k - T^*)(\Gamma_k - \tau)V^2$$

$$k = 1, 2, \ldots, n \qquad (7)$$

Putting $D_k \equiv \sqrt{[(X^* - x_k)^2 + (Y^* - y_k)^2]} = V(T_k - T^*)$, we finally have

$$(X^* - x_k)\alpha + (Y^* - y_k)\beta + VD_k\tau = VD_k\Gamma_k$$

$$k = 1, 2, \ldots, n \qquad (8)$$

This system of n simultaneous linear equations in 3 unknowns can be written in matrix notation

$$A\underline{x} = \underline{b} \qquad (9)$$

where $A = (a_{ij})$, $\quad i = 1, 2, \ldots, n, \quad j = 1, 2, 3$

$a_{i1} = (X^* - x_i)$,

$a_{i2} = (Y^* - y_i)$,

$a_{i3} = VD_i$,

$\underline{x} = (\alpha, \beta, \tau)^T$, and

$\underline{b} = (VD_1\Gamma_1, VD_2\Gamma_2, \ldots, VD_n\Gamma_n)^T$.

When Equation (9) is over-determined (i.e., $n > 3$), then multiply it by $A^T$ and solve :

$$(A^TA)\underline{x} = A^T\underline{b} \qquad (10)$$

which is a system of 3 simultaneous linear equations in 3 unknowns and can be solved by Gauss elimination method.

Since P-times can usually be determined to the nearest 0.1 s, we allow the errors $\Gamma_k$ ($k = 1, 2, 3, \ldots, n$) to take on 3 different states :

$$\Gamma_k = \begin{cases} -0.05 \text{ s} \\ 0 \text{ s} \\ +0.05 \text{ s} \end{cases} \qquad k = 1, 2, \ldots, n$$

For n stations, there are altogether $3^n$ combinations of the P-time errors and solving Equations (9) or (10) for these $3^n$ combinations, we get a set of results $\{\alpha_i, \beta_i, \tau_i\}$ ($i = 1, 2, \ldots, 3^n$). The distance errors in the x and y directions $\alpha_i$, $\beta_i$ can be combined to yield a resultant distance error :

$$\delta_i = \sqrt{[\alpha_i^2 + \beta_i^2]}, \qquad i = 1, 2, \ldots, 3^n \qquad (11)$$

The standard resultant distance error $\sigma_\delta$ and standard origin time error $\sigma_\tau$ are then given by

$$\sigma_\delta = [\Sigma_i\, \delta_i^2/3^n]^{1/2} \qquad i = 1, 2, \ldots, 3^n \qquad (12)$$

$$\sigma_\tau = [\Sigma_i\, \tau_i^2/3^n]^{1/2} \qquad i = 1, 2, \ldots, 3^n \qquad (13)$$

In the present study, the standard errors are computed for epicentres at the vertices of a 2 km grid system encompassing the area

$$-100 \text{ km} \leq x, y \leq 100 \text{ km}$$

with ROHq at the origin ($x = y = 0$ km). In other words, 101 x 101 = 10,201 grid points are considered.

The x and y coordinates for the stations (ROHq, YNF, TBT, CC) are computed from their latitudes and longitudes by using formulae (Lee and Stewart, 1981) derived by a method described by Richter (1958).

The above methodology can be easily extended to the case in which both P- and S-times are considered. The only change is to add the following n equations to the system of equations in (5) :

$$(X^* - x_k)^2 + (Y^* - y_k)^2 = V_s^2(T_k - T^*)^2$$

$$k = 1, 2, \ldots, n \qquad (14)$$

where $V_s = 5.6/1.78 = 3.15$ km/s and $T_k$ ($k = 1, 2, \ldots, n$) are the S-times. The corresponding errors $\Gamma_k$ ($k = 1, 2, \ldots, n$) can take on the same values for the P-times, or if the S-times can only be determined to the nearest second, then $\Gamma_k$ can take on the following 3 states instead :

$$\Gamma_k = \begin{cases} -0.5 \text{ s} \\ 0 \text{ s} \\ +0.5 \text{ s} \end{cases} \qquad k = 1, 2, \ldots, n$$

## 4. RESULTS OF ERROR ANALYSIS

### P-times at 3 Stations : YNF, TBT, CC

The error field for $\sigma_\delta$ is represented by a contour plot in Figure 1. It is obvious that while the standard distance errors are relatively small within the triangle formed by these three stations, there are 6 narrow strips for which the errors are very large ($\sigma_\delta$ > 100 km). On close examinations, these 6 strips lie along the external extensions of the mentioned triangle.

If we consider Equation (9), it can be shown that (in Appendix I) two out of the three rows of matrix A become dependent for points lying on the mentioned external extensions, rendering the solution of (9) indeterminate. In view of this, we may expect very large errors in locating epicentres in the vicinity of these 6 lines.

To show that there are indeed very large errors in locating epicentres in the vicinity of these 6 lines, let us consider an epicentre at point A with x = 56 km, y = 32 km (at 65 km east-northeast of ROHq) which lies on the east-northeast external extension formed by CC and YNF. The theoretical P-times (origin time = 0 s) are :

| | |
|---|---|
| YNF | 8.2 s |
| TBT | 13.2 s |
| CC | 14.9 s |

Incidentally, for an epicentre at point B with x ≈ 721 km, y ≈ 248 km (at 762 km east-northeast of ROHq), the corresponding theoretical P-times (origin time = -124.5 s) are :

| | |
|---|---|
| YNF | 8.2 s |
| TBT | 13.2 s |
| CC | 14.8 s |

which agree with those for point A within the error limit ±0.05 s. This means that no method can distinguish these two epicentres within observation errors and so a distance error of 699 km can result! This example also demonstrates that the solution of the epicentre location problem can be very sensitive to small changes in the P-times for a 3-station network.

Figure 2 shows a contour plot of the error field for $\sigma_t$. Its pattern is similar to that of $\sigma_\delta$ and the values are approximately 1/V (V = 5.6 km/s) of those for $\sigma_\delta$. This reflects the fact that the resultant distance errors are mainly due to distance errors in the radial directions. In view of this and since the main concern is location error, the standard origin time error fields are not considered for the remaining cases.

### P-times at 4 Stations : ROHq, YNF, TBT, CC

The error field for $\sigma_\delta$ is shown in Figure 3. It can be seen that when the P-time at ROHq is available, the errors are in general reduced compared with the previous case. However, there remain two narrow strips, one in the east-northeast and the other in the west-southwest direction, for which the errors are still fairly large. Noting that the 3 stations ROHq, YNF, and CC almost lie on a straight line and following the argument in the previous case, we expect matrix A in Equation (9) to become ill-conditioned for points on these two narrow strips and hence give rise to large errors.

Similar to the previous case, we can also show that there are indeed very large location errors for the 4-station network. Let us consider point A again. The theoretical P-times (origin time = 0 s) are now :

| | |
|---|---|
| ROHq | 11.5 s |
| YNF | 8.2 s |
| TBT | 13.2 s |
| CC | 14.9 s |

Incidentally, for an epicentre at point C with x $\approx$ 513 km, y $\approx$ 187 km (at 546 km east-northeast of ROHq), the corresponding theoretical P-times (origin time = -85.9 s) are :

| | |
|---|---|
| ROHq | 11.5 s |
| YNF | 8.2 s |
| TBT | 13.1 s |
| CC | 14.8 s |

which agree with those for point A within the error limit $\pm$0.05 s. This means that no method can distinguish these two epicentres within observational errors and so a distance error of 483 km can result!

**P-times at 4 Stations : ROHq, YNF, TBT, CC**
**S-time (Accuracy 0.1 s) at ROHq**

The error field for $\sigma_\delta$ is shown in Figure 4. It is obvious that if the S-time at ROHq is available to the nearest 0.1 s, the location errors are significantly reduced compared with the previous cases in which only P-times are used. Actually, $\sigma_\delta$ is less than 2 km within 100 km of ROHq. If we consider Equation (9), it is not difficult to understand that this significant reduction in the standard distance errors is due to the fact that matrix A will never become ill-conditioned if S-time(s) is/are included.

**P-times at 4 Stations : ROHq, YNF, TBT, CC**
**S-time (Accuracy 1 s) at ROHq**

The error field for $\sigma_\delta$ is shown in Figure 5. It can be seen that even if the S-time at ROHq is only available to the nearest 1 s, the errors are still significantly reduced compared with the cases in which only P-times are used. Due to larger S-time errors, the standard distance errors are larger than those in the previous case, especially for distances less than 40 km and in the vicinity of YNF, TBT and CC. Nevertheless, the errors are less than 4 km within 100 km of ROHq.

**P- and S-times at 4 Stations : ROHq, YNF, TBT, CC**
**S-time Accuracy 0.1 s**

Due to limited computer resources and in view of the fact that matrix A in Equation (9) will not become ill-conditioned when S-times are also used, a lower resolution of 10 km is used for the grid system in this and the following case.

The error field for $\sigma_\delta$ is shown in Figure 6. It can be seen that if S-times at all 4 stations are available to the nearest 0.1 s, the errors are even smaller compared with the case in which only the S-time at ROHq is available to the nearest 0.1 s. Indeed, the errors are less than 1 km within 100 km of ROHq.

**P- and S-times at 4 Stations : ROHq, YNF, TBT, CC**
**S-time Accuracy 1 s**

The error field for $\sigma_\delta$ is shown in Figure 7. The pattern resembles that of Figure 6 but the errors are in general larger by a factor of around 5. Nevertheless, the errors are still less than 4 km within 100 km of ROHq.

However, these errors are in general slightly larger than those for the case in which only the S-time at ROHq is available to the nearest 1 s (Figure 5). This shows that the error in epicentre determination is not always reduced by increasing the number of input (S-times in this case). More input with large errors can result in poorer solution.

## Summary and Remarks

From the above 6 cases, it can be seen that for the RO short-period seismograph network (3 or 4 stations), no matter what algorithm one adopts for epicentre determination, there are significant location errors for epicentres outside the network if only P-times are used. For some directions, earthquakes which occur at large distances may be located close to Hong Kong.

The location errors can be greatly reduced if accurate P- and S-times are both available. In case when we can only determine the S-time for ROHq to the nearest 1 s, $\sigma_\delta$ is in general less than or equal to 3 km within 100 km of ROHq. However, if S-times cannot be accurately determined, more S-time input can result in poorer solution.

Although the standard distance errors are in general only a few kilometres within 100 km of ROHq when accurate S-times are available, this study has not taken into account of the errors in adopting a crustal model. In fact, for a given error in the P- and/or S-velocities, location errors are expected to increase more for epicentres at larger distances from the stations due to longer travel times.

# 5. PERFORMANCE OF HYPO71PC

## Focal Depth Fixed at 0 km

Following Ginn (1988), theoretical arrival times at ROHq, YNF, TBT, CC for epicentres within 100 km of ROHq at 16 compass bearings were input into HYPO71PC and the program's output epicentre locations were compared with the actual positions. In order to demonstrate the usefulness of S-times, the following four cases were considered :

(a) P-times (accuracy 0.1 s) at 4 stations,
S-time (accuracy 0.1 s) at ROHq,
(b) P-times (accuracy 0.1 s) at 4 stations,
S-time (accuracy 1 s) at ROHq,
(c) P-times (accuracy 0.1 s) at 4 stations,
S-times (accuracy 0.1 s) at 4 stations, and
(d) P-times (accuracy 0.1 s) at 4 stations,
S-times (accuracy 1 s) at 4 stations.

Due to limited computer resources and for comparison with Ginn (1988), only the simple case of assuming one horizontal crustal layer with P-velocity 5.6 km/s and zero focal depth was considered. $V_p/V_s$ was taken to be 1.78.

The absolute distance errors of case (a) is shown in Table 1. For comparison, the absolute distance errors of EPILOC87 for 4 P-times input are reproduced in Table 2. It is obvious that the errors of HYPO71PC are significantly less than those of EPILOC87, especially at large distances. In fact, the errors of HYPO71PC are all less than 1 km while those of EPILOC87 can be up to 36 km (12 km) within 100 km (70 km) of ROHq.

The absolute distance errors of cases (b) to (d) are shown in Tables 3 - 5 respectively. It can be seen that with 4 S-times of accuracy 0.1 s, the errors are the smallest and they are all less than 1 km within 100 km of ROHq. If the S-times can only be determined to the nearest second, the errors increase. Nevertheless, the errors are still less than 4 km, with the largest error (3.3 km) obtained for case (b) at 80 km north-northeast of ROHq. These results are in general agreement with the findings in Section 4.

## Focal Depth not Fixed

In comparing the performance of HYPO71PC and EPILOC87 above, hypocentres with zero focal depth were considered and HYPO71PC was executed with focal depth fixed at 0 km. To assess the effect of non-zero focal depths on the performance of HYPO71PC, theoretical arrival times at ROHq, YNF, TBT, CC for epicentres with focal depth at 15 km and within 100 km of ROHq at 16 compass bearings were input into the program and output hypocentre locations were compared with the actual positions.

The four cases (a) - (d) were considered. For simplicity, the absolute distance errors of case (d) are shown in Table 6 since those of the other three cases are less. Comparing with Table 5, it can be seen that the errors are in general only slightly larger than those pertaining to fixed focal depth (0 km) with the largest one being 4 km at 90 km west of ROHq. Therefore, HYPO71PC still performs well in locating epicentres of earthquakes with non-zero focal depths.

Tables 7 and 8 show the absolute focal depth errors pertaining to cases (a) and (d) respectively. While the errors of the former case vary from 0.1 km to 6.9 km, those of the latter case can be up to 15 km. Also, errors are relatively small for short epicentral distances but they tend to increase with the distance from ROHq. Therefore, HYPO71PC can determine focal depth accurately only when reliable P- and S-times are both available and the epicentre lies close to the network.

**3-Station Network**

Under normal circumstances, P-times at the four short-period seismograph stations are available. Nevertheless, it is interesting to investigate the effect on the performance of HYPO71PC when P-time at one of the 3 outstations at YNF, TBT, and CC is not available due to failure of equipment or communication links.

To put HYPO71PC into stringent test, it was executed using only 3 P-times (1 from ROHq, 2 from the remaining 3 stations; accuracy 0.1 s) and 1 S-time (ROHq; accuracy 0.1 s or 1 s) as input. It was found that in many cases, even though the S-time at ROHq was available to the nearest 0.1 s, HYPO71PC yielded large errors.

Consider the case of an epicentre at 60 km southwest of ROHq. With 3 P-times (accuracy 0.1 s) from ROHq, YNF and TBT, and 1 S-time (accuracy 0.1 s) from ROHq as input, *HYPO71PC computed the epicentre at 34 km north of ROHq, implying a distance error* of 26 km and direction error of 140°! To understand why this happened, the root-mean-square of the P- and S-time residues for the case is plotted in Figure 8. It can be seen that while the global minimum lies at 60 km southwest of ROHq, there is another local (not global) minimum at around 30 to 40 km north of ROHq, the location which HYPO71PC obtained for the epicentre. In fact, the reason for the failure of HYPO71PC lies with the initial guess of the epicentre. In the program, location of the station with the earliest P-arrival is taken as the initial guess. However, in doing so, the Gauss-Newton iterative procedure (Section 2) ended up finding this local minimum instead of the global minimum.

Nevertheless, it should be noted that this deficiency of HYPO71PC can only be revealed by cases having poor station distribution and coverage. In fact, when the P-time at CC is also available in the above case, the residue field (Figure 9) only has one local (and hence global) minimum and HYPO71PC has no difficulty in locating the epicentre correctly.

In cases having poor station distribution and coverage, the problem can be overcome by choosing different initial guesses. In this way, the location of the global minimum residue can be determined by comparing the residues of the corresponding epicentres obtained by HYPO71PC. For our area of interest, the initial guesses can be taken from the vertices of the 10' grid system -100 km $\leq$ x,y $\leq$ 100 km. Using these initial guesses, HYPO71PC was executed again for the above cases. In this case, it was found that the distance errors were all below 1 km (4 km) for S-time accuracy of 0.1 s (1 s). These results are indeed similar to those obtained earlier.

## 6. VERIFICATION OF HYPO71PC USING ACTUAL EARTHQUAKE DATA

As explained in Section 3, the assumptions of a constant P-velocity and zero focal depth made in EPILOC87 are not realistic. In fact, various one-dimensional multi-layer crustal models derived from earthquake and rock blasting data are available. Two models, namely the Jeffreys and Bullen (J-B) model and the State Seismological Bureau (SSB) model, will be described. Using these models, HYPO71PC will be verified using seismic data obtained from earthquakes which occurred at Heyuan, Guangdong.

### The Jeffreys and Bullen (J-B) Model

The J-B model is the basis for the J-B Seismological Tables (Jeffreys and Bullen, 1940) which are still in use for epicentre determination by various seismological centres, including the International Seismological Centre (ISC) and the National Earthquake Information Centre (NEIC), USGS. The model was developed by Jeffreys in 1937 based on historical European near-earthquake studies (Bullen, 1963)

Basically, P- and S-velocities and layer thicknesses are specified for the upper crust, intermediate layers and upper mantle :

| | Upper crust | Intermediate layers | Upper Mantle |
|---|---|---|---|
| Thickness | 15 km | 18 km | — |
| $V_p$ | 5.57 km/s | 6.50 km/s | 7.76 km/s |
| $V_s$ | 3.36 km/s | 3.74 km/s | 4.36 km/s |

### The State Seismological Bureau (SSB) Model

The SSB model was derived by Guo et al (1981) of the Institute of Geophysics, SSB, China. Earthquake data collected in China and its bordering region during 1952 - 1971 and observations of large explosions were used. The model structure is similar to that of J-B but different values were obtained for the P- and S-velocities as well as the layer thicknesses :

| | Upper crust | Intermediate layers | Upper Mantle |
|---|---|---|---|
| Thickness | 16 km | 24 km | — |
| $V_p$ | 5.70 km/s | 6.51 km/s | 8.01 km/s |
| $V_s$ | 3.38 km/s | 3.75 km/s | 4.50 km/s |

The major differences between the two models are the depth of the intermediate layers [18 km (J-B) versus 24 km (SSB)] and $V_p$ for the upper mantle [7.76 km/s (J-B) versus 8.01 km/s (SSB)]. The former difference results in a significant difference in the crustal depth [33 km (J-B) versus 40 km (SSB)] while there is a 3 % difference in the latter one.

Looking at a seismotectonic map of Asia prepared by the Institute of Geology, SSB, China (SSB, 1981), the depth of the Mohorovicic discontinuity over the South China coastal region is less than 35 km whereas it is above 35 km for most parts of China (Figure 10). Therefore, although the crustal depth in the SSB model is applicable to most parts of China, it seems that the J-B model is more realistic for Hong Kong in this regard.

### Data

To verify HYPO71PC using actual earthquake data, we need to identify earthquakes which occurred close to Hong Kong and were significant enough so that their

seismic phases on the RO seismograms could be analyzed. The epicentral locations of these earthquakes as determined by international centres should also be available as a reference. Since the establishment of the RO network in 1979, 5 significant earthquakes which occurred at Heyuan were recorded by the network and located by the International Seismological Centre (ISC) and/or USGS. The arrival times at the RO stations and the epicentral locations as determined by ISC/USGS are listed in Table 9.

## Results

HYPO71PC was executed using the above-mentioned data set. In HYPO71PC, it is necessary to assume a constant $V_p/V_s$. In this respect, both J-B and SSB models suggest that the $P^*$ and $S^*$ waves (waves refracted from the Conrad Discontinuity) should be the first arrivals for earthquakes which occurred at Heyuan and therefore $V_p/V_s$ was taken to be $6.50/3.74 (\approx 6.51/3.75) = 1.74$.

Assuming that the ISC/USGS epicentral locations are exact, distance and bearing errors of HYPO71PC were computed and are summarized in Table 10. Two cases were examined :

(a) Both P- and S-times are input, and
(b) Only P-times are input.

The effect of adopting different crustal models will also be compared.

From Table 10, it is obvious that the results obtained by using both P- and S-times in locating the earthquakes at Heyuan are far more accurate than those obtained by using P-times only. In fact, while the root-mean-square distance and bearing errors for the former case are around 11 km and 4° respectively, the corresponding values for the latter case are around 136 km and 6°. In other words, without S-times, HYPO71PC located these earthquakes at about 30 to 40 km north of ROHq. In fact, this is also the case for EPILOC87 (see Section 1).

Table 10 also shows the effect of adopting different crustal models. Results obtained by using the RO assumptions of a constant P-velocity of 5.6 km/s and zero focal depths are also included for comparison. Considering the case of having both P- and S-times input, it can be seen that the errors pertaining to both J-B and SSB models are similar (9 km for distance; 4° for bearing) while those obtained by using the RO assumptions are somewhat larger (15 km for distance; 4° for bearing).

## Summary and Remarks

The above results show that if both P- and S-times of the RO network are available, HYPO71PC can locate earthquakes at Heyuan fairly accurately. However, without S-times as input, HYPO71PC, and in fact any epicentre determination program, yields unreliable locations with epicentral distances seriously underestimated for these earthquakes.

Adopting different crustal models affects the results slightly. It is apparent that the J-B and SSB models are more realistic than the RO assumptions. Since the SSB model may not be totally applicable to the South China coastal region, the J-B model can be adopted for Hong Kong until data become available to modify the parameters in the future.

Although the focal depths for these Heyuan earthquakes were also computed by HYPO71PC, they do not agree well with ISC/USGS data (not shown). Nevertheless, this inadequacy did not significantly affect the computed epicentre locations and is consistent with the findings in Section 5.

## 7. ADAPTATION OF HYPO71PC FOR REAL-TIME APPLICATION

Before putting HYPO71PC into operational use, the input data file for executing the program has to be customized in light of previous discussions. A sample input data file is included in Appendix II for reference. Detailed explanations of the input data format can be found in Lee (1989) or Lee and Lahr (1975). Essential input parameters are discussed briefly in the following two paragraphs.

The following data are essential for real-time application :

(a) Latitudes and longitudes of the seismograph stations

(b) P-velocity and depth for each crustal layer

As explained in Section 6, the J-B crustal model can be adopted for Hong Kong as a start.

(c) Ratio $V_p/V_s$

It is necessary to assume a constant $V_p/V_s$ ratio in HYPO71PC. Depending on the epicentral distance (which can be estimated by the S-P duration), the ratio can take on the values 1.66, 1.74, or 1.78 which corresponds to whether the first arrivals are ($P_g$, $S_g$), ($P^*$, $S^*$), or ($P_n$, $S_n$) respectively (Jeffreys and Bullen, 1940; Willmore, 1979).

(d) P- and S-times

P- and S-times can be typed into the input data file following the format specified in Lee (1989) or Lee and Lahr (1975). Nevertheless, if the earthquake concerned was recorded by the IASPEI PC-based Seismic Data Acquisition System (Lee, 1989), the P- and S-times input having the required HYPO71PC format can be prepared by using an analysis program known as PCEQ.

The sample input file in Appendix II shows the case of a locally felt earthquake which occurred near Mai Po on 6 December 1983. As a post-analysis, P- and S-times at Guangzhou and Macau were also input. The corresponding output is shown in Appendix III.

The first part of the output file displays all the input data so that the user can check whether there is any mistake in the input. The second part starts with essential parameters of the final solution, namely the date, origin time, latitude and longitude of epicentre, and focal depth. Other useful parameters are also given to help the user to assess the reliability of the solution. These include the azimuthal gap (largest azimuthal separation between stations), root-mean-square of the P- and S-time residues, standard errors of epicentre and focal depth, and solution quality of hypocentre. These are followed by station output which includes the epicentral distance for each station, azimuthal angle between epicentre and station (measured from north with respect to epicentre; bearing from station can be obtained by subtracting 180 degrees from the azimuthal angle), P- and S-times and the corresponding residues. Finally, root-mean-squares of the P- and S-time residues at 10 points on a sphere centred on the final hypocentre are shown in a 3-dimensional diagram. This diagram enables the user to determine whether or not the solution has converged to a minimum. Detailed explanations of the output can be found in Lee (1989) or Lee and Lahr (1975).

# 8. CONCLUSIONS

Regardless of the algorithm adopted to locate local earthquakes which occur outside a seismograph network, large errors can result if only P-times are used. These errors can be significantly reduced if accurate P- and S-times are both available.

A realistic crustal model is also required for accurate epicentre determination. Verification results obtained using actual seismic data suggest that the J-B model can be adopted for the South China coastal region.

In order to take the above conclusions into account, EPILOC87 is not adequate for reliable epicentre determination and programs such as HYPO71PC should be used instead.

## 9. ACKNOWLEDGEMENT

The author would like to thank Messrs C.K. Pan and M.S. Chau for their untiring efforts in computer programming and in preparation of the report.

## REFERENCES


| | | |
|---|---|---|
| Bullen, K.E. | 1963 | "An Introduction to the Theory of Seismology". Cambridge University Press, Cambridge. |
| Ginn, W.L. | 1988 | Report on Epicentre Determination (unpublished manuscript). |
| Guo, L.C. et al | 1981 | P and S Travel Times from Earthquakes in the Chinese Region, Acta Seismologica Sinica Vol. 3 No. 2, pp. 197 - 210. |
| Jeffreys, H. and Bullen, K.E. | 1940 | "Seismological Tables". Brit. Ass., Gray Milne Trust, London. |
| Lee, W.H.K. and Lahr, J.C. | 1972 | HYPO71 : A Computer Program for Determining Hypocenter, Magnitude, and First Motion Pattern of Local Earthquakes, U.S. Geol. Surv. Open-File Report. |
| Lee, W.H.K. and Lahr, J.C. | 1975 | HYPO71 (REVISED) : A Computer Program for Determining Hypocenter, Magnitude, and First Motion Pattern of Local Earthquakes, U.S. Geol. Surv. Open-File Report 75-311. |
| Lee, W.H.K. and Stewart, S.W. | 1981 | "Principles and Applications of Microearthquake Networks", Advances in Geophysics, Supplement 2. Academic Press, New York. |
| Lee, W.H.K. and Valdes, C.M. | 1985 | HYPO71PC : A Personal Computer Version of the HYPO71 Earthquake Location Program, U.S. Geol. Surv. Open-File Report 85-749. |
| Lee, W.H.K., Editor | 1989 | "Toolbox for Seismic Data Acquisition, Processing, and Analysis", IASPEI Software Library, Volume 1. Seismological Society of America, El Cerrito, CA. |
| Poon, H.T. | 1985 | "Seismological Measurements in Hong Kong", Proceedings of Conference on Geological Aspects of Site Investigation Bulletin No. 2, Geological Society of Hong Kong, August 1985. |
| Richter, C.F. | 1958 | "Elementary Seismology". Freeman, California. |
| State Seismological Bureau | 1978 | "近震分析", 地震出版社。 |
| State Seismological Bureau | 1981 | Seismotectonic Map of Asia and Europe. |
| Willmore, P.L. | 1979 | "Manual of Seismological Observatory Practice", WDC-A Report SE-20. |

## APPENDIX I

Consider a network of 3 stations with coordinates $(x_1, y_1)$, $(x_2, y_2)$, and $(x_3, y_3)$. Then matrix A in Equation (9) becomes :

$$\begin{bmatrix} X-x_1 & Y-y_1 & V\sqrt{[(X-x_1)^2+(Y-y_1)^2]} \\ X-x_2 & Y-y_2 & V\sqrt{[(X-x_2)^2+(Y-y_2)^2]} \\ X-x_3 & Y-y_3 & V\sqrt{[(X-x_3)^2+(Y-y_3)^2]} \end{bmatrix}$$

Now, suppose point (X, Y) lies on one of the external extensions formed by stations 1 and 2. Then X and Y satisfy the equation :

$$\frac{Y-y_1}{X-x_1} = \frac{Y-y_2}{X-x_2} = m$$

where $m = \dfrac{y_2-y_1}{x_2-x_1}$

and $(X-x_1)(X-x_2) > 0$

Therefore,

$$Y-y_1 = m(X-x_1)$$

$$Y-y_2 = m(X-x_2)$$

$$V\sqrt{[(X-x_1)^2+(Y-y_1)^2]} = V\sqrt{[(1+m^2)(X-x_1)^2]}$$

$$= V \mid X-x_1 \mid \sqrt{[1+m^2]}$$

$$V\sqrt{[(X-x_2)^2+(Y-y_2)^2]} = V\sqrt{[(1+m^2)(X-x_2)^2]}$$

$$= V \mid X-x_2 \mid \sqrt{[1+m^2]}$$

Now, if $X-x_1 > 0$ and $X-x_2 > 0$, then matrix A becomes

$$\begin{bmatrix} X-x_1 & m(X-x_1) & V\sqrt{[1+m^2](X-x_1)} \\ X-x_2 & m(X-x_2) & V\sqrt{[1+m^2](X-x_2)} \\ X-x_3 & Y-y_3 & V\sqrt{[(X-x_3)^2+(Y-y_3)^2]} \end{bmatrix}$$

and rows 1 and 2 of A are dependent.

If $X-x_1 < 0$ and $X-x_2 < 0$, then matrix A becomes

$$\begin{bmatrix} X-x_1 & m(X-x_1) & -V\sqrt{[1+m^2](X-x_1)} \\ X-x_2 & m(X-x_2) & -V\sqrt{[1+m^2](X-x_2)} \\ X-x_3 & Y-y_3 & V\sqrt{[(X-x_3)^2+(Y-y_3)^2]} \end{bmatrix}$$

and again rows 1 and 2 of A are dependent.

As this argument is valid for any 2 stations out of the 3, we can conclude that when point (X, Y) lies on one of the 6 external extensions of the triangle formed by these 3 stations, 2 out of the 3 rows of matrix A will become dependent and so the solution for Equation (9) in Section 3 is not unique.

# APPENDIX II
# SAMPLE INPUT DATA FILE FOR HYPO71PC

```
HEAD                                    EARTHQUAKE AT MAI PO (6 DECEMBER 1983)
RESET TEST( 1)=  0.5
RESET TEST( 2)= 30.0
RESET TEST( 3)=  0.0
RESET TEST( 6)=  1.0
RESET TEST(11)= 20.0
RESET TEST(13)=  5.0

  HKCV2218.21N11410.31E  29
  YHKV2222.75N11420.12E  87
  THKV2229.27N114 0.56E   4
  CHKV2212.17N114 1.46E  73
  MCO 22 7.38N11333.66E 158
  GZH 23 5.22N11320.63E  11

  5.57   0.00
  6.50  15.00
  7.76  33.00

   5.  50. 500. 1.66    4    1          0    1          0 11
HKCV P 1 831206142530.8         34.2  S 2
YHKV P 1 831206142531.6         35.7  S 2
THKV P 1 831206142527.2         28.5  S 1
CHKV P 1 831206142531.8         35.7  S 2
MCO  P 1 831206142536.3         44.1  S 1
GZH  P 1 831206142540.4         51.0  S 1
                 10
```

# APPENDIX III
# SAMPLE OUTPUT FILE OF HYPO71PC

EARTHQUAKE AT MAI PO (6 DECEMBER 1983)

***** PROGRAM: HYPO71PC (Version 1: 11/29/85) *****

| | TEST(1) | TEST(2) | TEST(3) | TEST(4) | TEST(5) | TEST(6) | TEST(7) | TEST(8) | TEST(9) | TEST(10) | TEST(11) | TEST(12) | TEST(13) |
|---|---|---|---|---|---|---|---|---|---|---|---|---|---|
| STANDARD | 0.1000 | 10.0000 | 2.0000 | 0.0500 | 5.0000 | 4.0000 | -0.8700 | 2.0000 | 0.0035 | 100.0000 | 8.0000 | 0.5000 | 1.0000 |
| RESET TO | 0.5000 | 30.0000 | 0.0000 | 0.0500 | 5.0000 | 1.0000 | -0.8700 | 2.0000 | 0.0035 | 100.0000 | 20.0000 | 0.5000 | 5.0000 |

| L | STN | LAT | LONG | ELV | DELAY | FMGC | XMGC | KL | PRR | CALR | IC | DATE | HRMN |
|---|---|---|---|---|---|---|---|---|---|---|---|---|---|
| 1 | HKCV | 2218.21N | 11410.31E | 29 | 0.00 | 0.00 | 0.00 | 0 | 0.00 | 0.00 | 0 | 0 | 0 |
| 2 | YHKV | 2222.75N | 11420.12E | 87 | 0.00 | 0.00 | 0.00 | 0 | 0.00 | 0.00 | 0 | 0 | 0 |
| 3 | THKV | 2229.27N | 114 0.56E | 4 | 0.00 | 0.00 | 0.00 | 0 | 0.00 | 0.00 | 0 | 0 | 0 |
| 4 | CHKV | 2212.17N | 114 1.46E | 73 | 0.00 | 0.00 | 0.00 | 0 | 0.00 | 0.00 | 0 | 0 | 0 |
| 5 | MCO | 22 7.38N | 11333.66E | 158 | 0.00 | 0.00 | 0.00 | 0 | 0.00 | 0.00 | 0 | 0 | 0 |
| 6 | GZH | 23 5.22N | 11320.63E | 11 | 0.00 | 0.00 | 0.00 | 0 | 0.00 | 0.00 | 0 | 0 | 0 |

CRUSTAL MODEL 1

| VELOCITY | DEPTH |
|---|---|
| 5.570 | 0.000 |
| 6.500 | 15.000 |
| 7.760 | 33.000 |

| KS | Z | XNEAR | XFAR | POS | IQ | KMS | KFM | IPUN | IMAG | IR | IPRN | CODE | LATR | | LONR | |
|---|---|---|---|---|---|---|---|---|---|---|---|---|---|---|---|---|
| 0 | 5. | 50. | 500. | 1.66 | 4 | 1 | 0 | 0 | 1 | 0 | 001100 | 0 | 0.00 | 0 | 0.00 | |

| DATE | ORIGIN | LAT N | LONG E | DEPTH | MAG | NO | DM | GAP | M | RMS | ERH | ERZ | Q | SQD | ADJ | IN | NR | AVR | AAR | NM | AVXM | SDXM | NF | AVFM | SDFM | I |
|---|---|---|---|---|---|---|---|---|---|---|---|---|---|---|---|---|---|---|---|---|---|---|---|---|---|---|
| 831206 | 1425 24.57 | 22-32.02 | 114- 1.54 | 12.67 | | 12 | 5 | 167 | 1 | 0.18 | 0.9 | 0.8 | C | B\|C | 0.07 | 10 | 12 | 0.00 | 0.13 | 0 | 0.0 | 0.0 | 0 | 0.0 | 0.0 | 5 |

| STN | DIST | AZM | AIN | PRMK | HRMN | P-SEC | TPOBS | TPCAL | DLY/HI | P-RES | P-WT | AMX | PRX | CALX | K | XMAG | RMK | FMP | FMAG | SRMK | S-SEC | TSOBS | S-RES | S-WT | DT |
|---|---|---|---|---|---|---|---|---|---|---|---|---|---|---|---|---|---|---|---|---|---|---|---|---|---|
| HKCV | 29.6 | 149 | 113 | P | 1 1425 | 30.80 | 6.23 | 5.78 | 0.00 | 0.45 | 0.56 | 0 | 0 | 0.00 | 0 | | | | | S | 2 34.20 | 9.63 | 0.04 | 0.4 | |
| YHKV | 36.2 | 118 | 109 | P | 1 1425 | 31.60 | 7.03 | 6.88 | 0.00 | 0.15 | 1.68 | 0 | 0 | 0.00 | 0 | | | | | S | 2 35.70 | 11.13 | -0.29 | 1.1 | |
| THKV | 5.3 | 198 | 157 | P | 1 1425 | 27.20 | 2.63 | 2.47 | 0.00 | 0.16 | 0.56 | 0 | 0 | 0.00 | 0 | | | | | S | 1 28.50 | 3.93 | -0.17 | 0.6 | |
| CHKV | 36.6 | 180 | 109 | P | 1 1425 | 31.80 | 7.23 | 6.96 | 0.00 | 0.27 | 0.56 | 0 | 0 | 0.00 | 0 | | | | | S | 2 35.70 | 11.13 | -0.42 | 0.4 | |
| MCO | 66.0 | 226 | 59 | P | 1 1425 | 36.30 | 11.73 | 11.76 | 0.00 | -0.03 | 1.62 | 0 | 0 | 0.00 | 0 | | | | | S | 1 44.10 | 19.53 | 0.00 | 1.6 | |
| GZH | 93.0 | 311 | 59 | P | 1 1425 | 40.40 | 15.83 | 15.92 | 0.00 | -0.09 | 1.52 | 0 | 0 | 0.00 | 0 | | | | | S | 1 51.00 | 26.43 | 0.00 | 1.5 | |

| | | | | | | |
|---|---|---|---|---|---|---|
| 34.75 | 4.46 | 7.67 | -0.73 | 0.88 | 0.69 | |
| 34.73 | 58.63 | 7.67 | -0.27 | 0.81 | | 0.62 |
| 34.73 | 4.46 | 17.67 | -0.69 | 0.75 | ( 0.57) | |
| 34.73 | 58.63 | 17.67 | -0.21 | 1.34 | | ( 1.16) |
| 32.02 | 1.54 | 4.01 | 0.00 | 0.79 | 0.61 | |
| | | | | 0.18 | 0.00 | |
| 32.02 | 1.54 | 21.33 | -0.11 | 0.43 | ( 0.25) | |
| 29.31 | 4.46 | 7.67 | 0.41 | 1.58 | 1.40 | |
| 29.31 | 58.63 | 7.67 | 0.64 | 0.90 | | 0.72 |
| 29.31 | 4.46 | 17.67 | 0.05 | 1.04 | ( 0.86) | |
| 29.31 | 58.63 | 17.67 | 0.42 | 0.94 | | ( 0.76) |

***** CLASS: A B C D TOTAL *****

NUMBER: 0.0 0.0 1.0 0.0 1.0

%: 0.0 0.0 100.0 0.0

| | TRAVELTIME RESIDUALS (MODEL=1) | | | | TRAVELTIME RESIDUALS (MODEL=2) | | | | X-MAGNITUDE RESIDUALS | | | F-MAGNITUDE RESIDUALS | | |
|---|---|---|---|---|---|---|---|---|---|---|---|---|---|---|
| STATION | NRES | SRWT | AVRES | SDRES | NRES | SRWT | AVRES | SDRES | NXM | AVXM | SDXM | NFM | AVFM | SDFM |
| HKCV | 1 | 0.56 | 0.45 | 0.00 | 0 | 0.00 | 0.00 | 0.00 | 0 | 0.00 | 0.00 | 0 | 0.00 | 0.00 |
| YHKV | 1 | 1.68 | 0.15 | 0.00 | 0 | 0.00 | 0.00 | 0.00 | 0 | 0.00 | 0.00 | 0 | 0.00 | 0.00 |
| THKV | 1 | 0.56 | 0.16 | 0.00 | 0 | 0.00 | 0.00 | 0.00 | 0 | 0.00 | 0.00 | 0 | 0.00 | 0.00 |
| CHKV | 1 | 0.56 | 0.27 | 0.00 | 0 | 0.00 | 0.00 | 0.00 | 0 | 0.00 | 0.00 | 0 | 0.00 | 0.00 |
| MCO | 1 | 1.62 | -0.03 | 0.00 | 0 | 0.00 | 0.00 | 0.00 | 0 | 0.00 | 0.00 | 0 | 0.00 | 0.00 |
| GZH | 1 | 1.52 | -0.09 | 0.00 | 0 | 0.00 | 0.00 | 0.00 | 0 | 0.00 | 0.00 | 0 | 0.00 | 0.00 |

Figure 1 Standard Distance Error Field
P-time Accuracy 0.1 s (3 stations)
No S-time

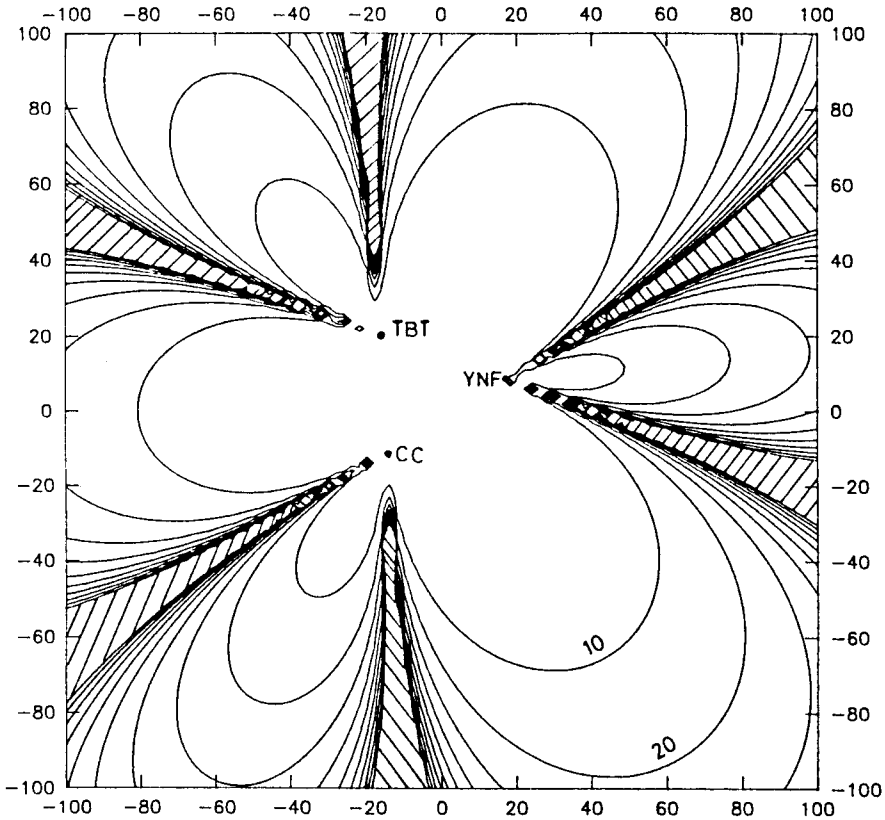


Error > 100 km

Error in km
Distance in km (from ROHq)

Figure 2 Standard Origin Time Error Field
P-time Accuracy 0.1 s (3 stations)
No S-time

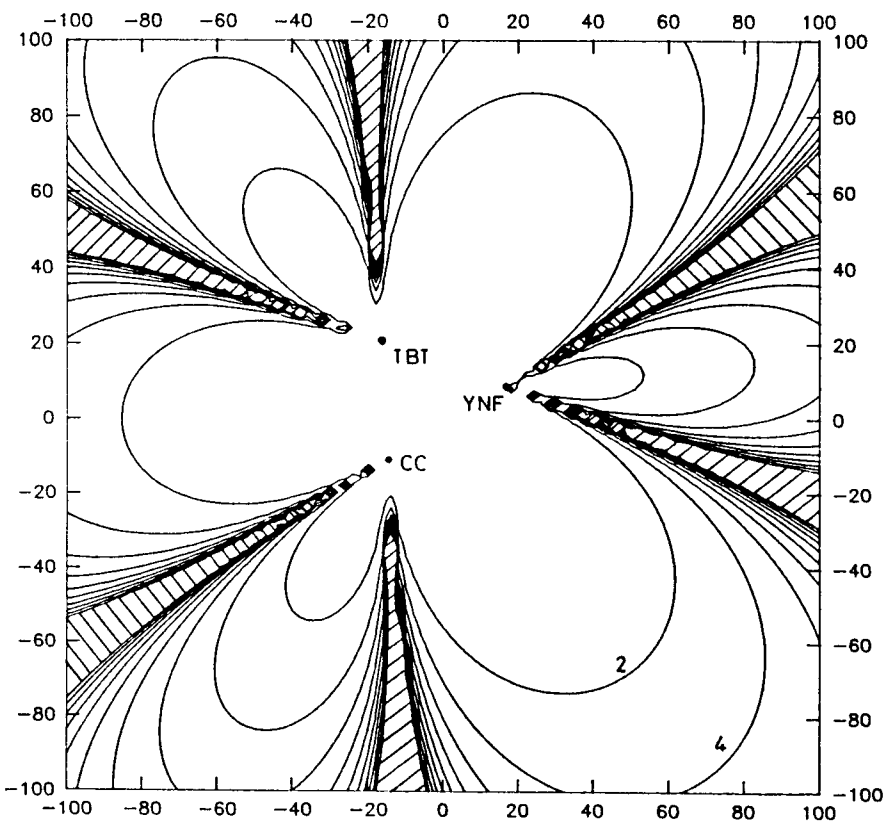


Error > 20 s

Error in s
Distance in km (from ROHq)

Figure 3 Standard Distance Error Field
P-time Accuracy 0.1 s (4 stations)
No S-time

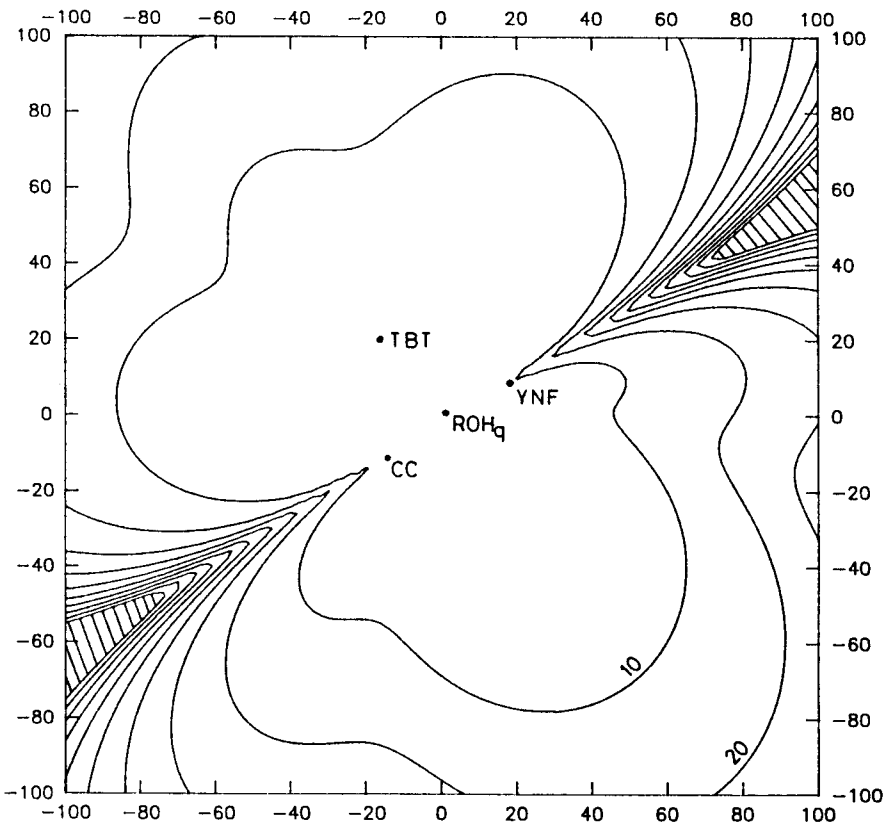


Error > 100 km

Error in km
Distance in km (from ROHq)

Figure 4 Standard Distance Error Field
P-time Accuracy 0.1 s (4 stations)
S-time Accuracy 0.1 s (ROHq only)

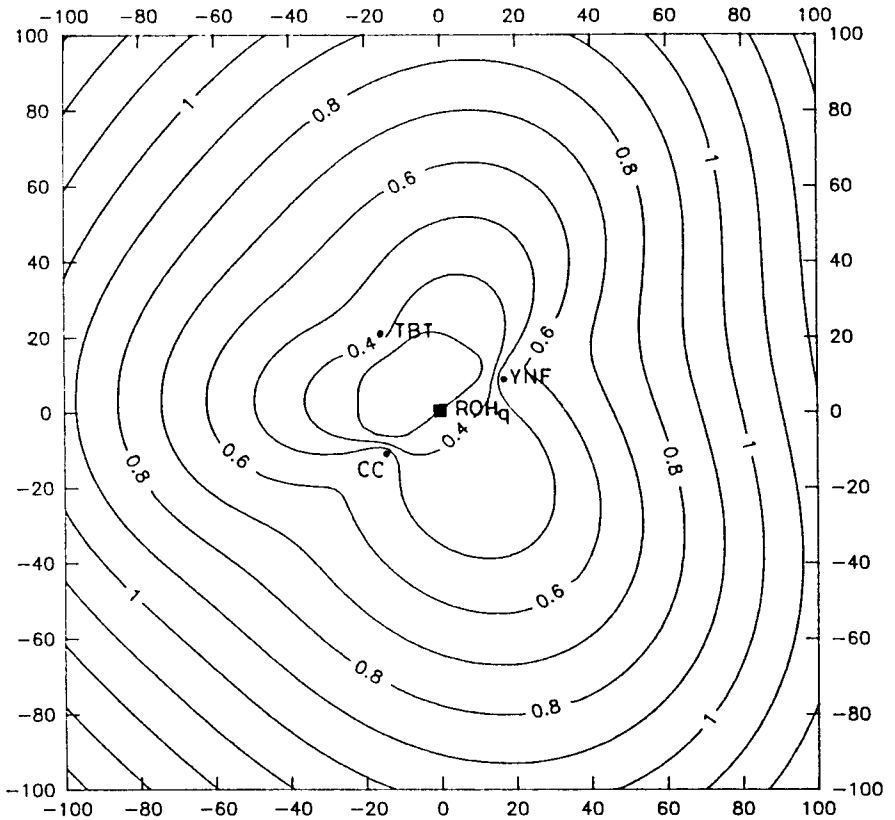


Error in km
Distance in km (from ROHq)

Figure 5 Standard Distance Error Field
P-time Accuracy 0.1 s (4 stations)
S-time Accuracy 1 s (ROHq only)

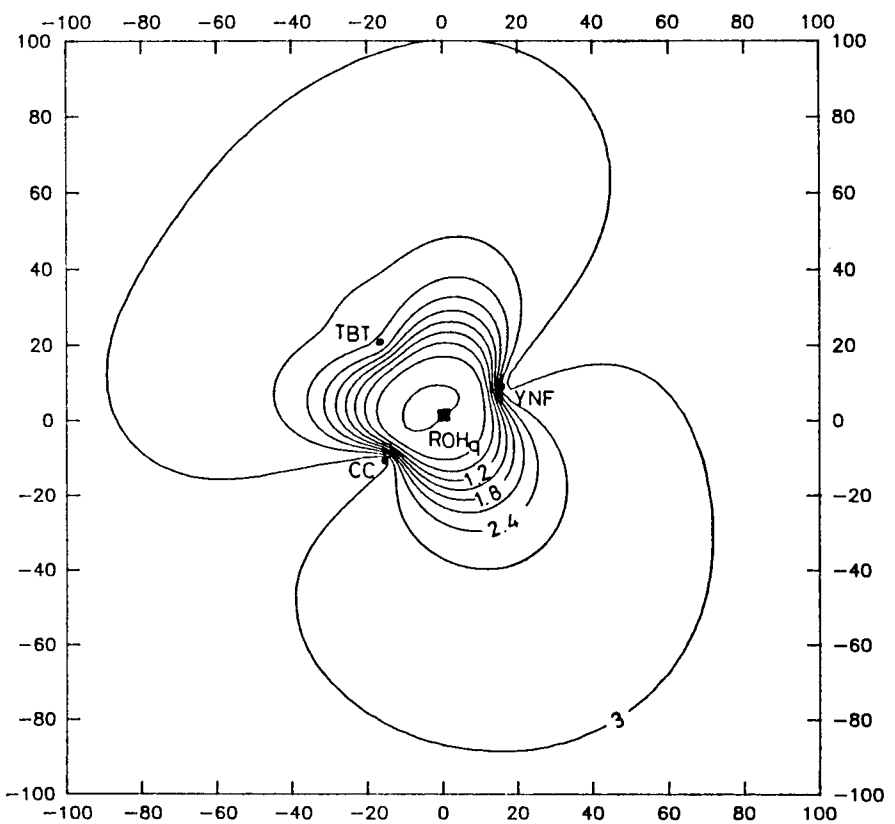


Error in km
Distance in km (from ROHq)

Figure 6 Standard Distance Error Field
P-time Accuracy 0.1 s (4 stations)
S-time Accuracy 0.1 s (4 stations)

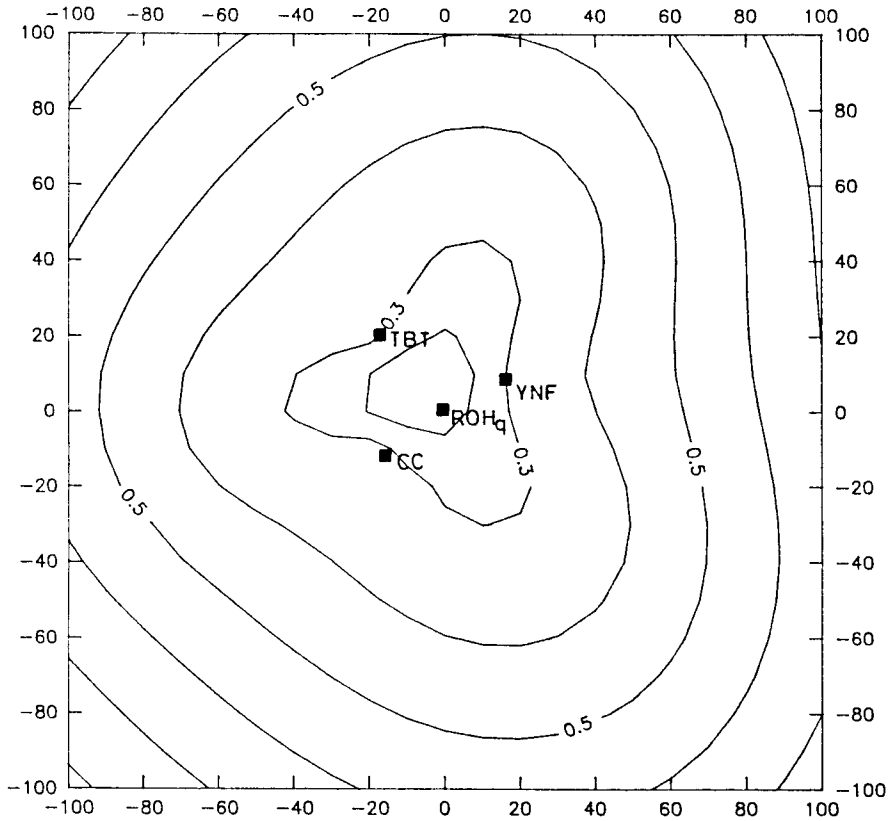


Error in km
Distance in km (from ROHq)

Figure 7 Standard Distance Error Field
P-time Accuracy 0.1 s (4 stations)
S-time Accuracy 1 s (4 stations)

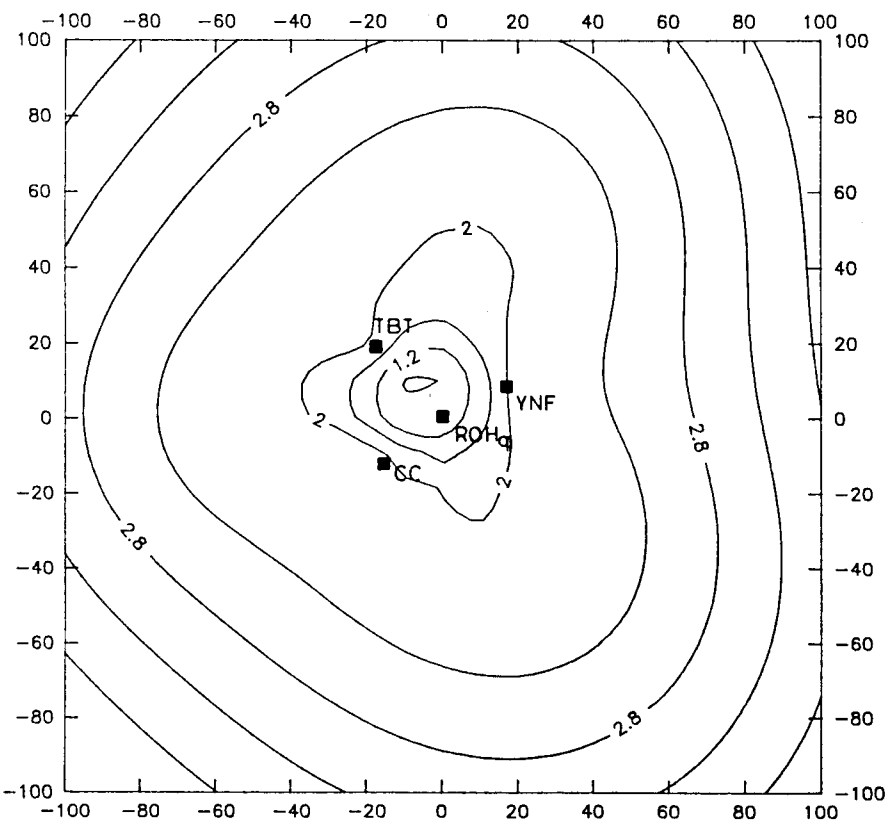


Error in km
Distance in km (from ROHq)

Figure 8 Residue Field SW 60 km
P-time Accuracy 0.1 s
(3 stations at ROHq, YNF & TBT)
S-time Accuracy 0.1 s (ROHq only)

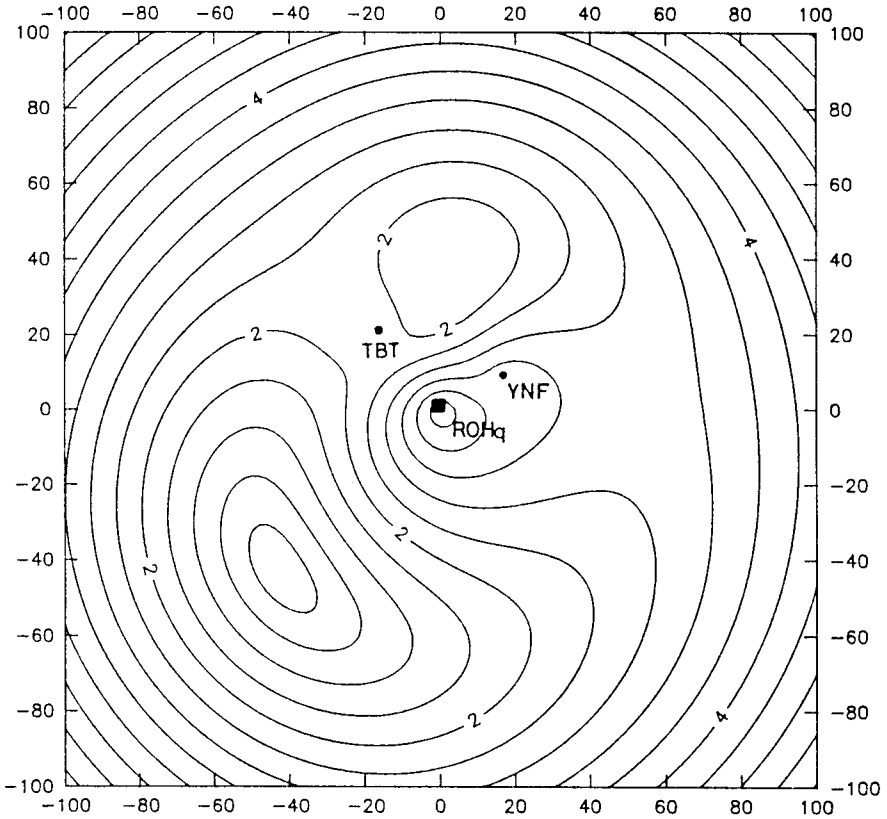


Residue in s
Distance in km (from ROHq)

Figure 9 Residue Field SW 60 km
P-time Accuracy 0.1 s (4 stations)
S-time Accuracy 0.1 s (ROHq only)

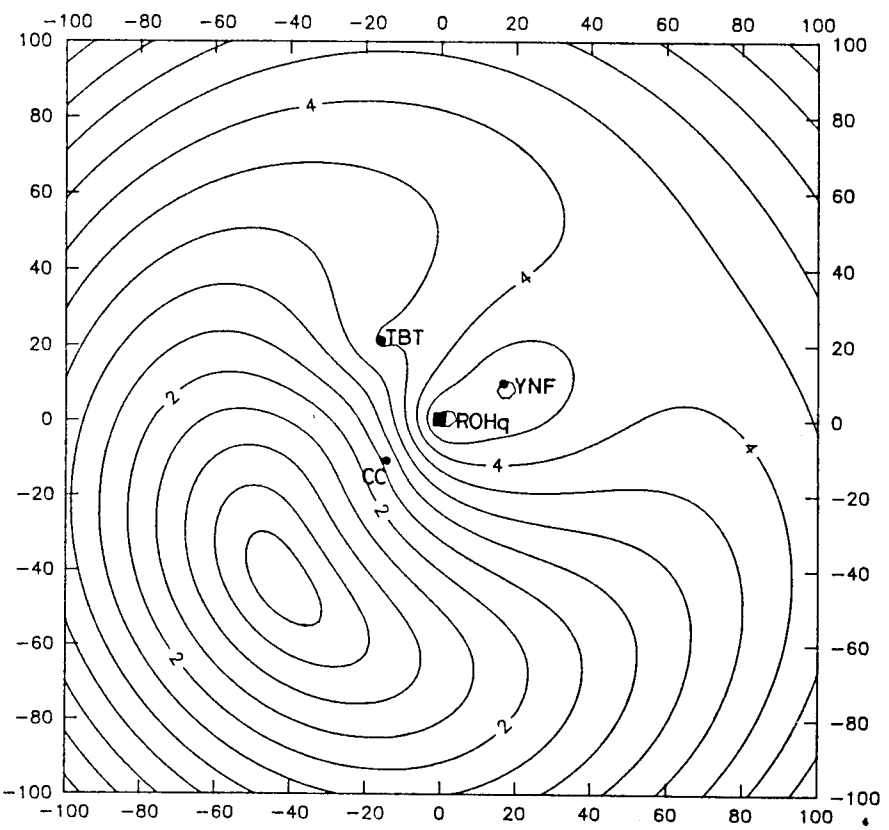


Residue in s
Distance in km (from ROHq)

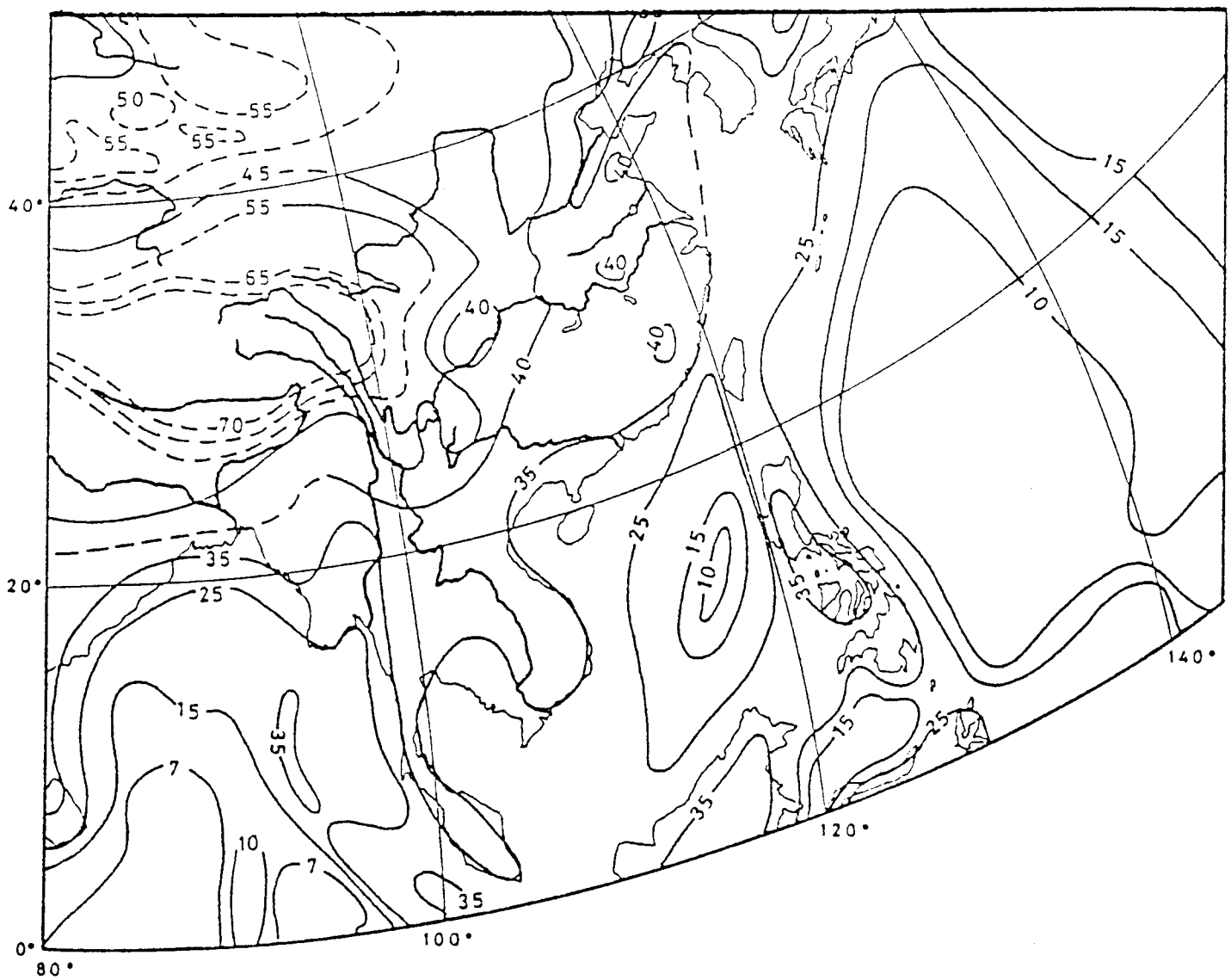


Figure 10 Depth of the Mohorovicic Discontinuity in East Asia in km
(Actual depths in solid lines, estimated depths in dotted lines)

**Table 1 : Absolute Distance Errors (km) of Case (a)**
**Focal Depth Fixed at 0 km**
**P-time Accuracy 0.1 s (4 Stations)**
**S-time Accuracy 0.1 s (ROHq Only)**

| DIST / DIR | Kilometers from ROHq | | | | | | | | | |
|---|---|---|---|---|---|---|---|---|---|---|
| | 10 | 20 | 30 | 40 | 50 | 60 | 70 | 80 | 90 | 100 |
| NNE | 0.1 | 0.2 | 0.2 | 0.0 | 0.0 | 0.1 | 0.3 | 0.5 | 0.1 | 0.0 |
| NE | 0.1 | 0.3 | 0.2 | 0.1 | 0.2 | 0.2 | 0.3 | 0.4 | 0.0 | 0.0 |
| ENE | 0.0 | 0.2 | 0.4 | 0.1 | 0.2 | 0.2 | 0.2 | 0.2 | 0.2 | 0.1 |
| E | 0.2 | 0.2 | 0.3 | 0.2 | 0.1 | 0.1 | 0.5 | 0.2 | 0.0 | 0.0 |
| ESE | 0.2 | 0.3 | 0.3 | 0.2 | 0.1 | 0.2 | 0.5 | 0.2 | 0.1 | 0.0 |
| SE | 0.1 | 0.0 | 0.0 | 0.0 | 0.1 | 0.2 | 0.4 | 0.3 | 0.0 | 0.1 |
| SSE | 0.1 | 0.1 | 0.2 | 0.1 | 0.1 | 0.4 | 0.3 | 0.2 | 0.1 | 0.0 |
| S | 0.0 | 0.3 | 0.3 | 0.1 | 0.2 | 0.2 | 0.4 | 0.3 | 0.1 | 0.0 |
| SSW | 0.1 | 0.1 | 0.3 | 0.1 | 0.0 | 0.4 | 0.3 | 0.3 | 0.0 | 0.0 |
| SW | 0.1 | 0.3 | 0.3 | 0.1 | 0.1 | 0.4 | 0.4 | 0.3 | 0.3 | 0.0 |
| WSW | 0.0 | 0.1 | 0.1 | 0.1 | 0.1 | 0.1 | 0.2 | 0.0 | 0.0 | 0.1 |
| W | 0.1 | 0.0 | 0.1 | 0.2 | 0.1 | 0.4 | 0.3 | 0.2 | 0.0 | 0.0 |
| WNW | 0.1 | 0.1 | 0.1 | 0.0 | 0.1 | 0.3 | 0.5 | 0.4 | 0.1 | 0.0 |
| NW | 0.2 | 0.1 | 0.3 | 0.0 | 0.1 | 0.4 | 0.5 | 0.3 | 0.0 | 0.1 |
| NNW | 0.2 | 0.1 | 0.1 | 0.2 | 0.1 | 0.1 | 0.4 | 0.1 | 0.1 | 0.3 |
| N | 0.1 | 0.0 | 0.1 | 0.0 | 0.0 | 0.1 | 0.5 | 0.2 | 0.2 | 0.2 |
| MEAN | 0.1 | 0.2 | 0.2 | 0.1 | 0.1 | 0.2 | 0.4 | 0.2 | 0.1 | 0.1 |
| MAX. | 0.2 | 0.3 | 0.4 | 0.2 | 0.2 | 0.4 | 0.5 | 0.5 | 0.3 | 0.3 |

**Table 2 : Absolute Distance Errors (km) of EPILOC87 (Ginn 1988)**
**Focal Depth Fixed at 0 km**
**P-time Accuracy 0.1 s (4 Stations)**
**No S-time**

| DIST / DIR | Kilometers from ROHq | | | | | | | | | |
|---|---|---|---|---|---|---|---|---|---|---|
| | 10 | 20 | 30 | 40 | 50 | 60 | 70 | 80 | 90 | 100 |
| NNE | 0.2 | 0.2 | 0.3 | 0.6 | 3.1 | 0.1 | 1.7 | 2.6 | 9.1 | 0.9 |
| NE | 0.3 | 0.5 | 0.8 | 1.0 | 4.0 | 4.1 | 4.2 | 10.0 | 23.2 | 35.5 |
| ENE | 0.2 | 0.2 | 5.0 | 2.0 | 3.9 | 1.5 | 0.3 | 1.2 | 15.1 | 9.2 |
| E | 0.0 | 0.5 | 4.0 | 2.0 | 1.5 | 11.5 | 3.0 | 23.0 | 13.0 | 5.0 |
| ESE | 0.2 | 0.2 | 0.2 | 1.9 | 1.7 | 5.5 | 6.4 | 3.6 | 17.8 | 7.8 |
| SE | 0.3 | 0.9 | 1.1 | 2.2 | 2.6 | 3.1 | 0.4 | 0.6 | 21.0 | 6.7 |
| SSE | 0.3 | 0.0 | 2.0 | 1.7 | 5.6 | 6.1 | 4.9 | 4.7 | 10.8 | 0.8 |
| S | 0.0 | 0.5 | 1.5 | 1.0 | 1.5 | 0.5 | 4.5 | 3.5 | 15.0 | 5.0 |
| SSW | 0.6 | 0.5 | 2.5 | 3.0 | 7.9 | 4.2 | 0.4 | 6.8 | 2.2 | 11.4 |
| SW | 0.1 | 4.8 | 0.3 | 1.7 | 0.1 | 4.4 | 1.1 | 2.4 | 6.5 | 28.1 |
| WSW | 0.1 | 0.0 | 2.2 | 0.7 | 4.0 | 5.4 | 8.4 | 13.2 | 24.8 | 14.2 |
| W | 0.0 | 0.0 | 0.5 | 1.5 | 0.0 | 4.5 | 4.0 | 8.5 | 4.0 | 5.0 |
| WNW | 0.3 | 0.0 | 1.8 | 0.6 | 0.4 | 2.3 | 2.7 | 0.4 | 21.8 | 11.8 |
| NW | 0.3 | 0.2 | 1.1 | 2.2 | 4.0 | 3.3 | 4.2 | 5.8 | 12.2 | 2.2 |
| NNW | 0.3 | 0.4 | 0.7 | 3.7 | 2.5 | 3.9 | 0.8 | 18.0 | 1.0 | 12.7 |
| N | 0.0 | 0.0 | 0.5 | 1.0 | 3.0 | 2.5 | 2.0 | 0.5 | 2.5 | 5.0 |
| MEAN | 0.2 | 0.6 | 1.5 | 1.7 | 2.9 | 3.9 | 3.1 | 6.6 | 12.5 | 10.1 |
| MAX. | 0.6 | 4.8 | 5.0 | 3.7 | 7.9 | 11.5 | 8.4 | 23.0 | 24.8 | 35.5 |

**Table 3 : Absolute Distance Errors (km) of Case (b)**
**Focal Depth Fixed at 0 km**
**P-time Accuracy 0.1 s (4 Stations)**
**S-time Accuracy 1 s (ROHq Only)**

| DIST / DIR | Kilometers from ROHQ | | | | | | | | | |
|---|---|---|---|---|---|---|---|---|---|---|
| | 10 | 20 | 30 | 40 | 50 | 60 | 70 | 80 | 90 | 100 |
| NNE | 0.2 | 1.0 | 2.4 | 1.9 | 0.6 | 0.6 | 1.8 | 3.3 | 2.8 | 1.4 |
| NE | 0.4 | 1.0 | 2.9 | 1.9 | 0.9 | 0.6 | 1.8 | 3.2 | 2.8 | 1.5 |
| ENE | 0.2 | 1.4 | 3.1 | 2.3 | 0.9 | 0.5 | 1.9 | 3.1 | 2.7 | 1.6 |
| E | 0.2 | 1.8 | 3.1 | 1.9 | 0.8 | 0.6 | 1.6 | 3.1 | 2.8 | 1.4 |
| ESE | 0.7 | 1.6 | 2.9 | 2.2 | 0.6 | 0.5 | 1.6 | 3.0 | 2.9 | 1.5 |
| SE | 0.5 | 1.9 | 3.1 | 2.0 | 0.8 | 0.5 | 1.7 | 3.1 | 2.8 | 1.3 |
| SSE | 0.5 | 1.8 | 2.9 | 2.0 | 0.6 | 0.2 | 1.8 | 3.0 | 2.9 | 1.4 |
| S | 0.5 | 1.7 | 2.9 | 2.1 | 0.9 | 0.5 | 1.7 | 3.2 | 2.9 | 1.4 |
| SSW | 0.3 | 1.9 | 3.1 | 2.2 | 0.7 | 0.3 | 1.8 | 3.1 | 2.8 | 1.4 |
| SW | 0.1 | 1.7 | 3.2 | 2.2 | 0.8 | 0.4 | 1.8 | 3.2 | 2.6 | 1.5 |
| WSW | 0.2 | 1.1 | 3.1 | 1.9 | 0.8 | 0.6 | 1.9 | 2.9 | 2.9 | 1.5 |
| W | 0.2 | 1.0 | 2.5 | 1.7 | 0.8 | 0.3 | 1.8 | 3.0 | 2.8 | 1.4 |
| WNW | 0.1 | 0.7 | 2.4 | 1.9 | 0.8 | 0.4 | 1.6 | 3.2 | 2.8 | 1.4 |
| NW | 0.0 | 0.3 | 2.8 | 2.0 | 0.6 | 0.3 | 1.5 | 3.1 | 2.8 | 1.3 |
| NNW | 0.0 | 0.5 | 2.7 | 1.8 | 0.8 | 0.6 | 1.7 | 2.9 | 2.8 | 1.7 |
| N | 0.1 | 1.0 | 2.4 | 1.8 | 0.7 | 0.5 | 1.6 | 3.0 | 2.6 | 1.6 |
| MEAN | 0.3 | 1.3 | 2.8 | 2.0 | 0.8 | 0.5 | 1.7 | 3.1 | 2.8 | 1.5 |
| MAX. | 0.7 | 1.9 | 3.2 | 2.3 | 0.9 | 0.6 | 1.9 | 3.3 | 2.9 | 1.7 |

**Table 4 : Absolute Distance Errors (km) of Case (c)**
**Focal Depth Fixed at 0 km**
**P-time Accuracy 0.1 s (4 Stations)**
**S-time Accuracy 0.1 s (4 Stations)**

| DIST / DIR | Kilometers from ROHq | | | | | | | | | |
|---|---|---|---|---|---|---|---|---|---|---|
| | 10 | 20 | 30 | 40 | 50 | 60 | 70 | 80 | 90 | 100 |
| NNE | 0.1 | 0.1 | 0.1 | 0.1 | 0.2 | 0.1 | 0.0 | 0.3 | 0.1 | 0.1 |
| NE | 0.1 | 0.2 | 0.1 | 0.2 | 0.1 | 0.1 | 0.2 | 0.1 | 0.1 | 0.1 |
| ENE | 0.0 | 0.2 | 0.2 | 0.2 | 0.2 | 0.0 | 0.1 | 0.0 | 0.1 | 0.0 |
| E | 0.1 | 0.1 | 0.1 | 0.1 | 0.0 | 0.0 | 0.2 | 0.1 | 0.1 | 0.0 |
| ESE | 0.1 | 0.0 | 0.2 | 0.2 | 0.1 | 0.2 | 0.3 | 0.1 | 0.0 | 0.0 |
| SE | 0.1 | 0.2 | 0.1 | 0.2 | 0.1 | 0.1 | 0.0 | 0.2 | 0.0 | 0.4 |
| SSE | 0.1 | 0.0 | 0.2 | 0.2 | 0.1 | 0.3 | 0.0 | 0.2 | 0.0 | 0.2 |
| S | 0.0 | 0.2 | 0.1 | 0.2 | 0.1 | 0.2 | 0.0 | 0.2 | 0.0 | 0.0 |
| SSW | 0.0 | 0.1 | 0.0 | 0.2 | 0.1 | 0.2 | 0.1 | 0.1 | 0.1 | 0.2 |
| SW | 0.0 | 0.1 | 0.3 | 0.3 | 0.0 | 0.3 | 0.0 | 0.1 | 0.2 | 0.2 |
| WSW | 0.0 | 0.0 | 0.0 | 0.1 | 0.3 | 0.1 | 0.1 | 0.1 | 0.0 | 0.1 |
| W | 0.0 | 0.0 | 0.1 | 0.0 | 0.0 | 0.4 | 0.0 | 0.2 | 0.0 | 0.0 |
| WNW | 0.0 | 0.0 | 0.0 | 0.0 | 0.1 | 0.1 | 0.4 | 0.2 | 0.1 | 0.3 |
| NW | 0.1 | 0.0 | 0.1 | 0.1 | 0.2 | 0.3 | 0.1 | 0.3 | 0.0 | 0.2 |
| NNW | 0.1 | 0.0 | 0.1 | 0.0 | 0.1 | 0.0 | 0.0 | 0.2 | 0.1 | 0.1 |
| N | 0.1 | 0.0 | 0.1 | 0.2 | 0.1 | 0.1 | 0.2 | 0.0 | 0.3 | 0.3 |
| MEAN | 0.1 | 0.1 | 0.1 | 0.1 | 0.1 | 0.2 | 0.1 | 0.2 | 0.1 | 0.1 |
| MAX. | 0.1 | 0.2 | 0.3 | 0.3 | 0.3 | 0.4 | 0.4 | 0.3 | 0.3 | 0.4 |

**Table 5 : Absolute Distance Errors (km) of Case (d)**
**Focal Depth Fixed at 0 km**
**P-time Accuracy 0.1 s (4 Stations)**
**S-time Accuracy 1 s (4 Stations)**

| DIST / DIR | Kilometers from ROHq | | | | | | | | | |
|---|---|---|---|---|---|---|---|---|---|---|
| | 10 | 20 | 30 | 40 | 50 | 60 | 70 | 80 | 90 | 100 |
| NNE | 0.5 | 0.5 | 0.8 | 0.0 | 0.4 | 0.9 | 0.3 | 0.8 | 0.4 | 1.5 |
| NE | 0.4 | 1.1 | 0.6 | 1.7 | 0.9 | 0.3 | 0.0 | 0.8 | 1.1 | 0.1 |
| ENE | 0.3 | 0.9 | 0.4 | 1.3 | 0.8 | 0.1 | 1.1 | 1.9 | 0.5 | 1.0 |
| E | 0.7 | 1.5 | 1.2 | 0.8 | 0.2 | 0.9 | 1.6 | 2.9 | 1.3 | 2.0 |
| ESE | 1.0 | 1.5 | 0.5 | 0.9 | 1.7 | 1.0 | 0.2 | 0.9 | 0.2 | 1.2 |
| SE | 0.7 | 1.0 | 2.5 | 0.5 | 0.0 | 0.8 | 0.1 | 1.0 | 0.1 | 1.2 |
| SSE | 1.2 | 0.1 | 2.2 | 0.8 | 0.0 | 0.3 | 1.3 | 1.3 | 2.4 | 1.1 |
| S | 0.5 | 0.8 | 1.1 | 0.0 | 0.7 | 1.5 | 2.4 | 1.5 | 1.6 | 1.8 |
| SSW | 0.9 | 0.3 | 0.9 | 0.9 | 0.1 | 0.6 | 1.7 | 0.7 | 0.2 | 2.2 |
| SW | 0.3 | 1.1 | 0.2 | 0.4 | 1.5 | 1.1 | 0.1 | 0.9 | 1.5 | 2.1 |
| WSW | 0.2 | 1.4 | 2.5 | 0.9 | 1.1 | 2.1 | 2.5 | 1.5 | 0.3 | 0.6 |
| W | 0.3 | 1.1 | 1.4 | 0.7 | 0.4 | 1.1 | 0.1 | 0.7 | 0.2 | 0.9 |
| WNW | 0.6 | 0.6 | 0.6 | 0.9 | 0.4 | 0.2 | 0.5 | 0.8 | 1.3 | 0.1 |
| NW | 0.4 | 0.0 | 0.3 | 0.3 | 0.6 | 0.5 | 0.2 | 1.4 | 0.9 | 2.2 |
| NNW | 0.2 | 0.1 | 0.5 | 0.8 | 1.0 | 0.4 | 0.2 | 0.6 | 2.0 | 1.2 |
| N | 0.0 | 0.6 | 1.6 | 0.1 | 0.1 | 0.4 | 0.7 | 1.7 | 0.8 | 2.1 |
| MEAN | 0.5 | 0.8 | 1.1 | 0.7 | 0.6 | 0.8 | 0.8 | 1.2 | 0.9 | 1.3 |
| MAX. | 1.2 | 1.5 | 2.5 | 1.7 | 1.7 | 2.1 | 2.5 | 2.9 | 2.4 | 2.2 |

**Table 6 : Absolute Distance Errors (km)**
**Focal Depth = 15 km (Not Fixed)**
**P-time Accuracy 0.1 s (4 Stations)**
**S-time Accuracy 1 s (4 Stations)**

| DIST / DIR | Kilometers from ROHq | | | | | | | | | |
|---|---|---|---|---|---|---|---|---|---|---|
| | 10 | 20 | 30 | 40 | 50 | 60 | 70 | 80 | 90 | 100 |
| NNE | 0.3 | 1.0 | 1.8 | 2.6 | 2.0 | 2.5 | 1.2 | 0.2 | 1.5 | 2.7 |
| NE | 0.6 | 0.2 | 0.4 | 0.7 | 0.8 | 0.4 | 1.0 | 0.3 | 0.9 | 2.3 |
| ENE | 0.3 | 0.1 | 0.2 | 1.3 | 1.1 | 1.2 | 1.7 | 0.8 | 0.2 | 0.7 |
| E | 0.8 | 0.1 | 1.7 | 3.2 | 2.9 | 2.7 | 1.8 | 1.4 | 0.6 | 0.9 |
| ESE | 0.6 | 0.0 | 0.2 | 0.2 | 1.5 | 1.9 | 1.2 | 1.9 | 2.0 | 1.9 |
| SE | 1.6 | 2.3 | 2.5 | 2.4 | 2.2 | 1.3 | 0.1 | 1.1 | 2.9 | 0.5 |
| SSE | 1.2 | 1.6 | 1.4 | 2.7 | 3.2 | 2.9 | 2.4 | 1.7 | 0.4 | 1.0 |
| S | 0.0 | 1.9 | 2.6 | 1.3 | 1.0 | 3.6 | 2.5 | 2.1 | 1.1 | 0.3 |
| SSW | 0.2 | 0.5 | 0.1 | 1.3 | 1.6 | 1.2 | 1.1 | 2.9 | 1.7 | 0.8 |
| SW | 0.6 | 0.0 | 0.3 | 2.4 | 0.3 | 0.7 | 1.1 | 2.4 | 1.6 | 0.7 |
| WSW | 0.5 | 0.3 | 0.5 | 0.5 | 0.6 | 0.6 | 2.7 | 2.3 | 1.5 | 0.6 |
| W | 0.5 | 0.4 | 1.0 | 1.6 | 1.2 | 1.0 | 0.5 | 0.3 | 4.0 | 2.4 |
| WNW | 1.3 | 0.0 | 0.8 | 1.6 | 1.4 | 1.6 | 1.3 | 0.2 | 1.6 | 0.5 |
| NW | 0.3 | 0.2 | 0.8 | 0.7 | 1.1 | 0.7 | 1.8 | 0.3 | 0.9 | 1.6 |
| NNW | 0.7 | 0.2 | 0.0 | 0.6 | 0.0 | 1.7 | 1.6 | 1.1 | 0.4 | 0.4 |
| N | 0.9 | 0.3 | 1.2 | 3.2 | 2.8 | 3.0 | 2.5 | 2.0 | 1.1 | 0.4 |
| MEAN | 0.7 | 0.6 | 1.0 | 1.6 | 1.5 | 1.7 | 1.5 | 1.3 | 1.4 | 1.1 |
| MAX. | 1.6 | 2.3 | 2.6 | 3.2 | 3.2 | 3.6 | 2.7 | 2.9 | 4.0 | 2.7 |

**Table 7 : Absolute Depth Errors (km)**
**Focal Depth = 15 km (Not Fixed)**
**P-time Accuracy 0.1 s (4 Stations)**
**S-time Accuracy 0.1 s (4 Stations)**

| DIST / DIR | Kilometers from ROHq | | | | | | | | | |
|---|---|---|---|---|---|---|---|---|---|---|
| | 10 | 20 | 30 | 40 | 50 | 60 | 70 | 80 | 90 | 100 |
| NNE | 0.3 | 0.3 | 0.3 | 0.5 | 0.3 | 1.2 | 0.5 | 1.6 | 2.3 | 3.0 |
| NE | 0.2 | 0.1 | 0.0 | 0.2 | 0.1 | 3.6 | 6.9 | 0.8 | 1.5 | 0.2 |
| ENE | 0.2 | 0.2 | 0.3 | 0.1 | 0.4 | 0.1 | 0.3 | 0.1 | 1.3 | 3.8 |
| E | 0.0 | 0.1 | 0.2 | 0.4 | 0.6 | 0.8 | 2.0 | 0.5 | 1.8 | 0.9 |
| ESE | 0.2 | 0.1 | 0.4 | 1.0 | 0.2 | 0.4 | 0.6 | 0.4 | 0.1 | 3.4 |
| SE | 0.1 | 0.6 | 0.1 | 0.7 | 0.4 | 2.1 | 1.1 | 1.1 | 0.3 | 3.1 |
| SSE | 0.1 | 0.1 | 0.0 | 1.0 | 0.1 | 1.5 | 0.2 | 0.3 | 0.7 | 2.2 |
| S | 0.3 | 0.6 | 0.4 | 0.1 | 0.1 | 0.1 | 1.6 | 0.3 | 2.7 | 2.0 |
| SSW | 0.2 | 0.2 | 0.2 | 0.4 | 0.1 | 0.2 | 0.5 | 1.0 | 2.2 | 1.5 |
| SW | 0.1 | 0.2 | 0.4 | 0.2 | 0.4 | 0.3 | 0.1 | 0.2 | 2.6 | 0.7 |
| WSW | 0.3 | 0.1 | 0.1 | 0.2 | 0.7 | 1.1 | 0.1 | 1.1 | 0.6 | 2.8 |
| W | 0.3 | 0.5 | 0.1 | 0.1 | 1.1 | 0.4 | 0.8 | 1.8 | 0.9 | 1.6 |
| WNW | 0.1 | 0.2 | 0.3 | 0.5 | 0.0 | 0.1 | 1.2 | 0.1 | 0.2 | 0.9 |
| NW | 0.0 | 0.2 | 0.1 | 0.1 | 0.2 | 0.5 | 0.9 | 1.6 | 0.5 | 3.4 |
| NNW | 0.5 | 0.3 | 0.1 | 0.1 | 0.3 | 0.6 | 0.4 | 1.2 | 0.6 | 1.9 |
| N | 0.0 | 0.0 | 0.1 | 0.1 | 0.7 | 0.2 | 1.0 | 1.3 | 3.6 | 0.6 |
| MEAN | 0.2 | 0.2 | 0.2 | 0.3 | 0.4 | 0.8 | 1.1 | 0.8 | 1.4 | 2.0 |
| MAX. | 0.5 | 0.6 | 0.4 | 1.0 | 1.1 | 3.6 | 6.9 | 1.8 | 3.6 | 3.8 |

**Table 8 : Absolute Depth Errors (km)**
**Focal Depth = 15 km (Not Fixed)**
**P-time Accuracy 0.1 s (4 Stations)**
**S-time Accuracy 1 s (4 Stations)**

| DIST / DIR | Kilometers from ROHq | | | | | | | | | |
|---|---|---|---|---|---|---|---|---|---|---|
| | 10 | 20 | 30 | 40 | 50 | 60 | 70 | 80 | 90 | 100 |
| NNE | 0.2 | 2.0 | 2.1 | 8.2 | 0.7 | 14.1 | 3.6 | 0.1 | 5.4 | 7.9 |
| NE | 1.6 | 0.9 | 1.4 | 1.4 | 2.5 | 2.5 | 11.7 | 14.6 | 4.5 | 7.8 |
| ENE | 2.4 | 0.7 | 0.4 | 1.8 | 0.3 | 3.7 | 9.3 | 8.3 | 10.1 | 10.6 |
| E | 1.1 | 2.0 | 1.2 | 3.0 | 1.0 | 0.6 | 0.1 | 0.8 | 1.1 | 2.4 |
| ESE | 1.8 | 0.8 | 2.0 | 1.6 | 5.7 | 9.1 | 0.7 | 0.2 | 14.0 | 2.9 |
| SE | 2.6 | 4.3 | 0.0 | 0.5 | 6.3 | 1.1 | 2.4 | 4.6 | 10.2 | 5.3 |
| SSE | 1.3 | 1.1 | 4.8 | 8.1 | 14.3 | 12.7 | 14.0 | 9.6 | 7.0 | 3.2 |
| S | 1.0 | 1.6 | 3.3 | 2.7 | 7.4 | 14.6 | 7.9 | 12.1 | 8.0 | 13.3 |
| SSW | 0.7 | 0.4 | 0.5 | 5.0 | 5.0 | 4.8 | 5.4 | 14.3 | 14.5 | 13.6 |
| SW | 2.0 | 0.6 | 0.1 | 3.1 | 0.1 | 2.2 | 4.2 | 14.4 | 14.4 | 14.4 |
| WSW | 0.6 | 0.2 | 0.4 | 4.2 | 2.3 | 7.5 | 14.4 | 13.8 | 13.9 | 13.8 |
| W | 0.2 | 0.9 | 1.5 | 0.1 | 0.7 | 5.9 | 2.6 | 1.7 | 11.1 | 4.0 |
| WNW | 0.1 | 0.7 | 3.6 | 0.7 | 4.3 | 9.7 | 10.8 | 5.0 | 2.2 | 6.8 |
| NW | 0.7 | 1.6 | 0.4 | 2.6 | 0.4 | 2.2 | 4.2 | 6.4 | 7.7 | 6.8 |
| NNW | 0.1 | 2.3 | 2.4 | 1.5 | 1.8 | 9.2 | 14.4 | 15.0 | 14.2 | 13.9 |
| N | 1.1 | 0.3 | 1.2 | 11.1 | 3.5 | 14.4 | 14.5 | 14.1 | 14.1 | 13.5 |
| MEAN | 1.1 | 1.3 | 1.6 | 3.5 | 3.5 | 7.1 | 7.5 | 8.4 | 9.5 | 8.8 |
| MAX. | 2.6 | 4.3 | 4.8 | 11.1 | 14.3 | 14.6 | 14.5 | 15.0 | 14.5 | 14.4 |

**Table 9 : Seismic Data for Verification of HYPO71PC**

| Date | Station | P-time | S-time | Location | Distance from ROHq (km) | Bearing |
|---|---|---|---|---|---|---|
| 810504 | ROHq | 110531.0 | 110550.0 | 23.82 N* | 177 | 18° |
| | YNF | 29.2 | 48.0 | 114.70 E | | |
| | TBT | 29.5 | 48.3 | | | |
| | CC | 33.0 | 57.2 | | | |
| 810608 | ROHq | 003641.0 | 003659.0 | 23.6 N* | 159 | 22° |
| | YNF | 39.3 | 57.4 | 114.8 E | | |
| | TBT | 39.5 | 58.0 | | | |
| | CC | 42.9 | 003707.4 | | | |
| 860915 | ROHq | 054756.7 | — | 24.02 N* | 192 | 8° |
| | YNF | 55.4 | 054817.1 | 114.43 E | | |
| | TBT | 54.7 | 13.5 | | | |
| | CC | 58.4 | 22.6 | | | |
| 870915 | ROHq | 020459.6 | — | 23.79 N* | 169 | 13° |
| | YNF | 57.8 | 020516.7 | 114.53 E | | |
| | TBT | 57.5 | 16.2 | | | |
| | CC | 020501.2 | 25.1 | | | |
| 891125 | ROHq | 161412.5 | 161430.8 | 23.72 N+ | 163 | 15° |
| | YNF | 10.8 | 28.4 | 114.58 E | | |
| | TBT | 10.9 | 28.7 | | | |
| | CC | 14.5 | 38.1 | | | |

* Located by ISC

\+ Located by USGS

**Table 10 : Verification Results of HYPO71PC**

**Distance (km) and Bearing (degrees in brackets) Errors (P- and S-times Input)**

| Date | Crustal Model | | |
|---|---|---|---|
| | J-B | SSB | RO* |
| 810504 | -15 ( 4) | -12 ( 4) | -19 ( 2) |
| 810608 | - 6 ( 2) | 5 ( 1) | - 4 (-1) |
| 860915 | - 8 (-6) | -14 (-7) | -22 (-7) |
| 870915 | - 7 ( 3) | - 1 ( 3) | -11 ( 2) |
| 891125 | - 5 ( 5) | - 9 ( 5) | -14 ( 5) |
| Root-Mean-Square | 9 ( 4) | 9 ( 4) | 15 ( 4) |

**Distance (km) and Bearing (degrees in brackets) Errors (Only P-times Input)**

| Date | Crustal Model | | |
|---|---|---|---|
| | J-B | SSB | RO* |
| 810504 | -143 (-5) | -143 (-5) | -145 (- 6) |
| 810608 | -118 (-8) | -118 (-8) | -129 (-11) |
| 860915 | -154 (-2) | -146 (-2) | -161 (- 4) |
| 870915 | -132 (-5) | -130 (-4) | -133 (- 5) |
| 891125 | -128 (-3) | -128 (-3) | -129 (- 4) |
| Root-Mean-Square | 136 ( 5) | 133 ( 5) | 140 ( 7) |

* RO stands for the simple model of assuming a constant P-velocity of 5.6 km/s and zero focal depths.